AD-A193 224 CREEP OF CARBON YARN AND CARBON-CARBON COMPOSITES AT HIGH TEMPERATURES AN.. (U) CALIFORNIA UNIV LOS ANGELES DEPT OF MATERIALS SCIENCE AND ENG.. G SINES ET AL.

UNCLASSIFIED MAY 88 UCLA-ENG-88-8 N00014-85-K-0667 F/G 11/2 NL

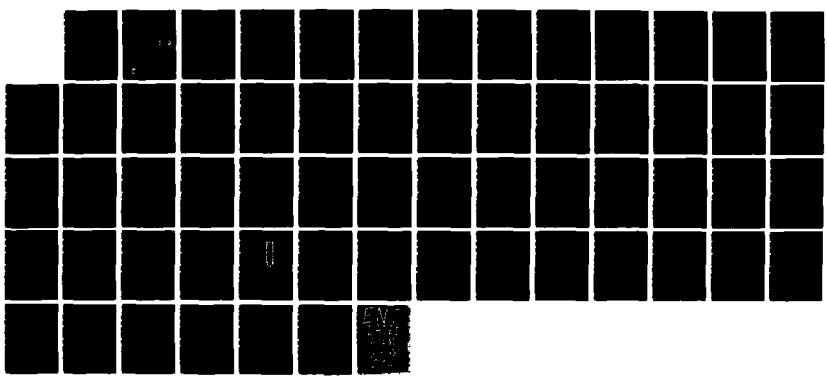

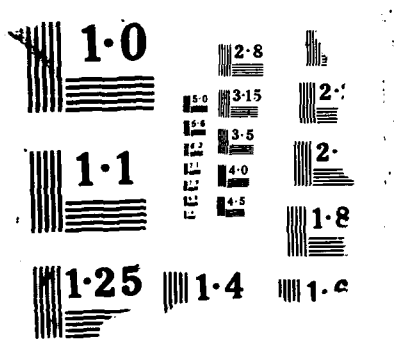
1·0
1·1
1·25
2·8
3·15
3·5
4·0
4·5
1·4
1·8

(4)

UCLA School of Engineering and Applied Science

CREEP OF CARBON YARN AND
CARBON-CARBON COMPOSITES AT
HIGH TEMPERATURES AND HIGH STRESSES

by George Sines, Zheng Yang and Brian D. Vickers

ONR-N00014-85-K-0667
L.H. Peebles, Monitor

UCLA-ENG-88-8
May 1988

UCLA SCHOOL OF ENGINEERING AND APPLIED SCIENCE

CREEP OF CARBON YARN AND CARBON-CARBON COMPOSITES

AT HIGH TEMPERATURES AND HIGH STRESSES

by
George Sines, Zheng Yang, and Brian D. Vickers

Department of Materials Science and Engineering
School of Engineering and Applied Science
University of California
Los Angeles

Technical Report

Prepared for
Department of the Navy
Office of Naval Research
Arlington, Virginia 22217

Monitor, Dr. L.H. Peebles, Jr.

Contract No. N00014-85-K-0667
Report No. UCLA-ENG-88-8

May 1988

SECURITY CLASSIFICATION OF THIS PAGE

REPORT DOCUMENTATION PAGE

1a. REPORT SECURITY CLASSIFICATION unclassified	1b. RESTRICTIVE MARKINGS
2a. SECURITY CLASSIFICATION AUTHORITY	3. DISTRIBUTION/AVAILABILITY OF REPORT unlimited
2b. DECLASSIFICATION/DOWNGRADING SCHEDULE	
4. PERFORMING ORGANIZATION REPORT NUMBER(S) UCLA-ENG-88-8	5. MONITORING ORGANIZATION REPORT NUMBER(S)
6a. NAME OF PERFORMING ORGANIZATION UCLA Dept of Mat Sci & Engr School of Engr & Applied Sci 6b. OFFICE SYMBOL (If applicable)	7a. NAME OF MONITORING ORGANIZATION Monitor, Dr. L.H. Peebles, Jr. Office of Naval Research
6c. ADDRESS (City, State, and ZIP Code) Los Angeles, Calif. 90024	7b. ADDRESS (City, State, and ZIP Code) Arlington, Virginia 22217
8a. NAME OF FUNDING/SPONSORING ORGANIZATION 8b. OFFICE SYMBOL (If applicable)	9. PROCUREMENT INSTRUMENT IDENTIFICATION NUMBER ONR-N00014-85-K-0667
8c. ADDRESS (City, State, and ZIP Code)	10. SOURCE OF FUNDING NUMBERS PROGRAM ELEMENT NO. / PROJECT NO. / TASK NO. / WORK UNIT ACCESSION NO

11. TITLE (Include Security Classification)

Creep of Carbon Yarn and Carbon-Carbon Composites at High Temperatures and High Stresses

12. PERSONAL AUTHOR(S)

George Sines, Zheng Yang, Brian D. Vickers

13a. TYPE OF REPORT	13b. TIME COVERED FROM ____ TO ____	14. DATE OF REPORT (Year, Month, Day)	15. PAGE COUNT
		May 1988	61

16. SUPPLEMENTARY NOTATION

17. COSATI CODES			18. SUBJECT TERMS (Continue on reverse if necessary and identify by block number)
FIELD	GROUP	SUB-GROUP	Carbon-Carbon Composites; Creep; Carbon Yarn; Creep-Behavior; Carbon Matrix; Creep Testing

19. ABSTRACT (Continue on reverse if necessary and identify by block number)

To better understand the creep-behavior of carbon yarn and carbon-carbon composites, creep experiments were developed that permitted testing at high temperatures (up to 2500 C) and at high stresses (up to 850 MPa) on specially prepared, uniaxial specimens that had a known gage length. Using a Dorn-type power law relation to model steady-state creep the apparent activation energy for the carbon yarn and carbon composite specimens was determined to be 1082 kJ/mol. This value represents a single thermally activated process, vacancy diffusion, that compares favorably with the energies determined or calculated by other researchers for various types of graphitizable carbon. The value determined for the stress exponent was 7.5. It too was found to be independent

(over)

20. DISTRIBUTION/AVAILABILITY OF ABSTRACT ☒ UNCLASSIFIED/UNLIMITED ☐ SAME AS RPT ☐ DTIC USERS	21. ABSTRACT SECURITY CLASSIFICATION unclassified
22a. NAME OF RESPONSIBLE INDIVIDUAL	22b. TELEPHONE (Include Area Code) / 22c. OFFICE SYMBOL

DD FORM 1473, 84 MAR 83 APR edition may be used until exhausted. All other editions are obsolete.

SECURITY CLASSIFICATION OF THIS PAGE

19. (continued)

of the carbon matrix's presence and independent of the specimens' loading history. Values of the pre-exponential constant for the carbon yarn and carbon composites were also calculated.

As stated in a previous report the carbon matrix greatly improves the creep resistance of the carbon composite. This improvement was attributed to the the matrix's microstructure. It distributes applied loads more evenly and it may also impose a triaxial stress state in the yarn's filaments. It is proposed that such a stress state may inhibit the flux of vacancies thus accounting in part for this increase in creep resistance. Another explanation, which states that only a fraction of the filaments in the matrix-free specimens are fully loaded during creep, is also considered.

Apparent activation volumes were calculated. Their magnitudes, 2088 $Å^3$ for the matrix-free specimen and 1583 $Å^3$ for the composite, suggest that diffusion occurs on a large, molecular size scale. Finally, a quantity which may be considered as the work required to activate the activation volume was derived and confirmed by the data.

ABSTRACT

To better understand the creep-behavior of carbon yarn and carbon-carbon composites, creep experiments were developed that permitted testing at high temperatures (up to 2500 C) and at high stresses (up to 850 MPa) on specially prepared, uniaxial specimens that had a known gage length. Using a Dorn-type power law relation to model steady-state creep the apparent activation energy for the carbon yarn and carbon composite specimens was determined to be 1082 kJ/mol. This value represents a single thermally activated process, vacancy diffusion, that compares favorably with the energies determined or calculated by other researchers for various types of graphitizable carbon. The value determined for the stress exponent was 7.5. It too was found to be independent of the carbon matrix's presence and independent of the specimens' loading history. Values of the pre-exponential constant for the carbon yarn and carbon composites were also calculated.

As stated in a previous report the carbon matrix greatly improves the creep resistance of the carbon composite. This improvement was attributed to the the matrix's microstructure. It distributes applied loads more evenly and it may also impose a triaxial stress state in the yarn's filaments. It is proposed that such a stress state may inhibit the flux of vacancies thus accounting in part for this increase in creep resistance. Another explanation, which states that only a fraction of the filaments in the matrix-free specimens are fully loaded during creep, is also considered.

Apparent activation volumes were calculated. Their magnitudes, 2088 $Å^3$ for the matrix-free specimen and 1583 $Å^3$ for the composite, suggest that diffusion

occurs on a large, molecular size scale. Finally, a quantity which may be considered as the work required to activate the activation volume was derived and confirmed by the data.

ACKNOWLEDGEMENTS

The authors would like to thank Leslie Feldman of The Aerospace Corporation for his thoughtful advice and Fred Weiler here at UCLA for his help with the equipment and instrumentation.

TABLE OF CONTENTS

LIST OF TABLES

LIST OF FIGURES

1. INTRODUCTION

Impressive thermal characteristics such as stability up to temperatures of 3000 C make carbon in its many forms a high temperature material par excellence [1,2]. One of the most useful and promising of these forms is high-strength, high-stiffness, carbon fibers. When used to form carbon composites these fibers, with their excellent mechanical properties, have enabled carbon to reach beyond its refractory capabilities and into the realm of structural applications. The aerospace industry has so far benefited the most from carbon-carbon's abilities. Some established high-temperature structural applications include: re-entry components such as nose cones and leading edges, rocket nozzles, exhaust cones, and templates for super-plastic forming of metals [1].

Since high temperatures and stresses are encountered by carbon-carbon composites during their fabrication and sometimes during their service [3], there is considerable interest in this material's creep behavior. The fabrication of three-dimensional, carbon-carbon composite billets is one example where a knowledge of this behavior would aid in preventing costly manufacturing errors [4,5]. These billets, with their highly anisotropic thermal and mechanical properties, (as woven into a network of bundles and matrix pockets), experience high internal stresses during processing due to repeated heatings to the high temperatures of graphitization [3]. These stresses are often so high that debonding of the carbon bundles and cracking of the billet - sometimes catastrophically - can occur [5].

Carbon-carbon research has invested a great deal of effort in trying to understand what happens to these composite billets during fabrication. Recent work performed

here at UCLA, (including this report and refs. 4,6,7), has been concerned with the creep behavior of carbon-carbon composites at high stress levels and at high temperatures - conditions representative of those experienced by the billets as they're being processed. It is felt that the information derived from these studies might be used to develop more effective time-temperature processing paths which would utilize creep to relax the stresses generated within the billets.

A great deal of work is available on high temperature processes such as graphitization and deformation for various types of carbon, graphite, and their fibers. Work concerned with carbon-carbon composite creep, however, is limited to only a few studies such as the prior work by the authors [7] and that reported by Feldman [8,9,10] which tested for uniaxial tensile creep in unimpregnated and pitch-impregnated (composite) carbon yarn. A distinguishing characteristic of the authors' initial tests was the high stress levels (770 MPa; 112 ksi) reached during experimentation. These high stress levels showed that the microstructure of the carbon matrix significantly enhances the yarn's resistance to creep deformation. This improvement in creep resistance was attributed to the matrix's ability to distribute loads more evenly and to the likely imposition of a plastic flow inhibiting, triaxial stress state in the well-bonded filaments of the carbon yarn. Testing at these stress levels also revealed that the creep response of the impregnated carbon yarn had a rather large primary stage [7].

This report is a continuation of the above work. Additional creep tests, which varied both the load and the temperature, have been performed. From these tests the apparent activation energy, the stress exponent, and the pre-exponential constant for both unimpregnated carbon yarn

and carbon composite yarn have been determined. These results were compared with those obtained by other investigators for pyrolytic carbons and graphites in an attempt to identify the thermally activated process. An explanation is also given why the carbon matrix is so influential in the creep resistance of the carbon fibers. The apparent activation volume as well as a theoretically derived quantity that may be considered as the work required to activate the apparent activation volume have also been determined in an effort to explain and characterize the materials' behavior.

2. EXPERIMENTAL

2.1 Materials

The materials used in the preparation of uniaxial, carbon-carbon composite specimens were the following: HM3000 polyacrylonitrile-based (PAN) yarn (Hercules) was used for fibers and 15V coal-tar pitch (Allied) was used as matrix precursor. The HM3000 yarn consist of 3000 filaments, each with a nominal diameter of 7 microns, and has a Young's modulus of 380 GPa (55 Msi) along the fiber's axis. The as-received yarn had a protective sizing on it which was removed thermally before the specimen was prepared. The pitch was also thermally pre-treated to remove many of the volatiles, prior to the specimen's impregnation. Manufacturers' data are presented in table 1.

2.2 Test Specimens

Figure 1 is a drawing of a test specimen. Details on its design, fabrication and heat treatment can be found in the previous report [7]. All specimens were slowly carbonized to 900 C before being tested for creep. Of note is the test section which provided a known gage length of one inch and the reinforced ends which permitted testing at high stress levels. There were two types of specimens used for creep testing: composite specimens which had an impregnated test section and specimens which had a matrix-free test section. All of the specimens' reinforced ends were impregnated with pitch and carbonized to provide strength for testing.

2.3 Apparatus

The high temperature creep tests were performed in a modified Astro furnace (model 2250), which had a graphite heating element. The furnace was controlled manually. Its temperature profile was approximately parabolic with the hot zone centered over the test section; short-time temperature fluctuations are estimated to be from 1 to 5 C and were quickly corrected manually. Changes in elongation were monitored by an LVDT (Schaevitz) which had DC inputs and outputs and a sensitivity of 0.50 mm/V. Furnace temperature was measured and controlled via an optical pyrometer (Honeywell). A loading beam was used to stabilize the load and the specimen. It consisted of a beam supported on knife edges on a frame anchored to the base of the furnace (the LVDT's output was amplified by its positioning on the loading beam away from the loading axis). An inert atmosphere of helium at a pressure of about 5 cm (2 in) of water was maintained during testing. Data was collected on an x-y recorder as elongation versus time. See figure 2 for a schematic of the test equipment and figure 3 for a detailed drawing of the apparatus. A more complete description concerning the design of the testing apparatus can also be found in the previous report [7].

2.4 Procedure

Each test specimen was hung vertically in the furnace between two graphite pin and clevis fixtures. Specimens were slowly heated to the desired initial test temperature and held there (this 'holding time' ranged from 10 to 20 min) while under a small pre-load of 272 g (0.6 lb). Application of test loads was slowly done in steps and without shock via the slow release of the loading beam. Thermal, elastic and creep responses were all recorded as

elongation versus time for both the composite and the matrix-free uniaxial test specimens.

Since there is often a great deal of scatter in creep results, a statistical method called the Chauvenet Criterion [11] was used to check if individual values were valid or not. As for different groups of results - specifically those of the composite specimens versus those of the 'dry' - a statistical method called the Sum of Ranks Test [12] was used to judge whether the results from one group were remarkably different from that of the others.

3. RESULTS AND DISCUSSION

3.1 Carbon Yarn Creep

Studies, such as the ones done by Hawthorne [13] on the stretch graphitization of vitreous carbon fibers and by Feldman on graphite fibers indicate a thermally activated, steady state creep rate $\dot{\varepsilon}$ which is dependent on the stress σ and the temperature T

$$\dot{\varepsilon} = A\sigma^n \exp(-Q/RT) \qquad \text{eqn. 1}$$

where n is the stress exponent, R is the gas constant, A is a pre-exponential factor, and Q is the apparent activation energy. This is one of the power-law forms of the Dorn equation for creep [see Poirier, 14, p.91]. It should be noted that Q, as determined from the slope of the plot of the logarithm of the strain rate versus inverse temperature does not account for any dependence that the shear modulus might have on the temperature, [eg., see Langdon, 15], and how this dependence may influence the mobility of atomic defects.

Equation 1 concentrates on the thermal response of the fibers which control the strength and stiffness of the composite. This is unlike most models used to describe the creep of continuous fiber composites which factor in (usually by some rule of mixtures) the contribution of the creeping matrix phase to the overall behavior [16]. This is not to imply that the carbon matrix is not important to the overall behavior. It just doesn't act as the composite's limiting phase because its melting point is not lower than that of the fibers and its mechanical properties are very poor when compared to those of the fibers.

3.2 Determining the Stress Exponent and Apparent Activation Energy from the Data

The value of the stress exponent n was determined from the slope of the plot of the logarithm of the steady-state strain rate versus the logarithm of the stress. Data were acquired via step-loading each specimen at a constant temperature. These steps were alternated between increasing and decreasing load increments to see if the creep behavior and the value of the stress exponent were dependent on the loading history. Steady-state strain rate values were obtained from the slope of the linear recording made between load steps. Schematics showing the type of loading used are presented in figure 4.

Stress values for both the matrix-free and the composite specimens were calculated using the net area of the carbon yarn. These calculations were based upon the assumption that the yarn carries almost all of the load in these composites. Since the diameter of the specimens are continuously decreasing during the creep deformation the stress data were corrected to represent the true stress.

$$\sigma = \sigma_o(1+\epsilon) \qquad \text{eqn.2}$$

where σ is the mean true stress at each load step, σ_o is the initial engineering stress, ($\sigma_o = P/A_o$; P is the applied load, A_o is the initial cross-sectional area of the yarn at the test section), and ϵ is the average engineering strain at each load step.

The apparent activation energy Q for creep deformation was determined from the slope of the plot of the logarithm of the steady-state strain rate versus the inverse temperature, (an Arrhenius plot). A schematic of a typical portion of the creep curve used to gather this constant stress data is shown in figure 5. Only increasing

temperature steps were performed. Since calculations for the data acquired here assumed a constant stress, the above stress corrections could not be made at each temperature step. Instead, a single, average corrected stress was used as determined between the beginning and the end of the increasing-temperature curve.

The creep test of a matrix-free ('dry') specimen which involved both step-loading and increasing temperature steps is shown in figure 6. After the desired test temperature was reached, held and deemed stabilized, an initial load was applied (t=0 in the graphs), and a transient response recorded. Each time that the deformation rate achieved a steady-state, the applied load was incrementally increased or decreased. This procedure was then followed by a period of increasing temperature steps until the end of the test. Thus, from each specimen, a value of the stress exponent and the apparent activation energy could be determined from a single trial. This data could then be used to calculate the pre-exponential constant A.

Four carbon composite specimens and five matrix-free ('dry') specimens were tested in this manner. Temperatures ranged from 2120 to 2430 C. Stresses ranged from 455 to 800 MPa (66 to 116 ksi), with the matrix-free specimens tested at the lower stress levels as they were less creep resistant. Two additional composite specimens were also tested at constant temperature and stress conditions. This was done to obtain a simplified perspective of the creep-behavior, as well as to determine if the time spent at the test temperature just prior to load application (the 'holding-time') would have any effect.

It should be noted that the initial thermal and elastic responses of the creep specimens, which were large, depended not only on the specimens' properties but also on the

compliance and expansion coefficient of the furnace and load train. Furthermore, the manner in which the specimens' end loops seated themselves on their pin and clevis fixtures during the initial loading affected the compliance and was surely different for each specimen. Because of these variables these initial responses provided no useful data.

3.3 Effect of Holding-Time

Graphitization of the fibers is a function of the heat treatment temperature [1] and also of the applied stress which accelerates the dewrinkling process [17]. By enhancing the preferred orientation, these processes improve the elastic modulus and also may improve the fiber's strength [18]. Because of these potential changes in mechanical properties, the decision was made to try and observe the effect that the holding time might have on the creep-behavior of the specimens.

Two composite specimens (G6 and G7) were prepared for comparison. They were tested under similar condition except for the time that they were held at the test temperature (2310 C) while under the pre-load (272g; 0.6 lbs). Specimen G6 was held only 5 minutes while specimen G7 was held for 1 hour. The results of these tests are shown in table 2. See figure 7 for a comparison of the two curves.

The results show that the composite specimen G7 was somewhat more creep resistant than G6, but not by a significant amount. This is not very surprising since HM3000, a PAN-based fiber, is already graphitized about as much as it can be at 2310 C. The interlayer distance d vs. HTT curves (ref. 1, p.171] for various carbon fibers show almost no decrease in d ($d = c/2 = 0.346$ nm) between 2100 and 2500 C for PAN-based fibers; though the fact that our

specimens were also highly stressed may have improved this value. Given that creep data is prone to scatter and that most specimens were held from 10 to 25 minutes, it is felt that spending more time at the holding temperature would not significantly change the mechanical properties of these specimens and thereby affect the results.

3.4 Creep Behavior of Carbon-Carbon Composites

The G6 and G7 curves (figure 7) also provide a good representation of the creep behavior of carbon composites at high temperatures and high stress levels. A rather large transient response is notable. After one hour the creep strain measured for these two trials is already a significant percentage (37 and 38 per cent) of the total deformation after six hours. This transient portion of the creep curve is most likely a combination of several mechanisms which act in concert with the thermally activated process. These mechanisms may include: graphitization, dewrinkling and sliding of fiber crystallites, and the collapse of fiber pores [see the structural models of carbon fibers presented in ref. 18].

With the decay of the transient response the steady-state response became apparent. This response at these high stress levels was very sensitive to any changes in the temperature. Fluctuations in the temperature of the furnace or even in the surrounding environment would register as small, but perceptible, deviations in the slope until the test temperature was re-established.

3.5 Apparent Activation Energy

The Arrhenius plots used to determine the apparent activation energy for the four composite and five matrix-free specimens are compiled in figure 8 while the data are presented in table 3. The average values of 1110 kJ/mol (265 kcal/mol) for the composite specimens and 1058 kJ/mol (253 kcal/mol) for the dry specimens were determined as not significantly different. Because of the excellent agreement between the values of Q for the two types of specimens, the conclusion is made that the same thermally activated process occurs in the carbon yarn regardless of the presence of the carbon matrix.

Tabulated lists that compare the experimental results of many researchers for high temperature creep and graphitization [see Hawthorne 13; Cannon 19, p.27; and Fischbach 17, p.65] show that for many pyrolytic carbons, graphites and cokes, the value of the apparent activation energy falls in the 960 to 1170 kJ/mol range (230 to 280 kcal/mol). Especially supportive were the values obtained by Granoff [20] for the graphitization of carbon-felt/CVD carbon-matrix composites (1005 and 1155 kJ/mol). The mean value of 1082 kJ/mol (258 kcal/mol) as determined from the nine creep tests in this report, is quite comparable to these results.

The activation energies for carbon atoms in graphite were theoretically calculated by Dienes [21] and then by Kanter [22] (see table 4). Their results, along with the evidence cited in the lists referenced above, indicate that there is a well-defined activation energy which is representative of a single high-temperature process [17]. This process involves the formation and motion of vacancies (vacancy controlled diffusion) and it is regarded as the primary mechanism during the graphitization and/or the high

temperatures deformation of graphitizable carbons. Since the results of the tests performed in this study on PAN-based carbon yarn and carbon-carbon composites compare favorably to the reported results of other carbon materials, the diffusion of vacancies is also regarded as the steady-state creep mechanism in these tests.

3.6 Diffusion in the Presence of the Matrix

In the previous report [7], it was reported that a matrix-free specimen ruptured with approximately 140% strain after only 0.39 hours of testing (constant temperature of 2310 C; constant stress of 770 MPa, 112 ksi). These results were significantly different than those of a composite specimen tested at the same conditions which endured only 3.6% strain after 5.9 hours without failure. As stated in section 3.5, the formation and motion of vacancies is regarded as the thermally activated creep mechanism in the carbon yarn - irrespective of the matrix. Yet as shown, the carbon matrix does wield considerable influence; its presence greatly improves the composite's creep resistance. This improvement was attributed to the alignment and proper bonding of the carbonaceous mesophase layers in the matrix. This type of microstructure creates a 'sheath effect' which more evenly distributes loads and which may also generate a triaxial stress state that inhibits plastic flow in the filaments of the carbon yarn.

This mechanical enhancement by the well-bonded matrix can possibly be related to the diffusion mechanism in the carbon yarns and composites by considering the effect that the stress state has on the shear stress. With the imposition of a triaxial stress state the shear stress is necessarily reduced (becoming zero for equal triaxial stresses). If the motion of defects relies on the magnitude

of the shear stress [14], then the carbon filaments of the dry specimens, which experience disproportionate, uniaxial stresses and hence a higher shear stress, have a greater flux of vacancies and therefore creep faster. This can explain why more load (perhaps much more) is needed to generate the same flux of vacancies in the composite specimens as that which caused the high deformation rates in the matrix-free specimens.

3.7 Apparent Activation Volume

The expression for the apparent activation volume as used by Hawthorne [13] for the stretch-graphitization of glassy carbon fibers was

$$V = 2kT\left(\frac{d\ln\dot{\varepsilon}}{d\sigma}\right) \qquad \text{eqn. 3}$$

where k is Boltzman's constant, T is the absolute temperature, $\dot{\varepsilon}$ is the steady state strain rate and σ is the applied stress. Ishai [23] regarded the quantity V_0 "as the volume of the activated segmental unit involved in the diffusion process" - a structural parameter which is the product of the interatomic distance λ_1, the intermolecular distance λ_2, and the jump distance λ_0. It should be noted that the expression used by Hawthorne and by some other authors to define the apparent activation volume considers only half the jump distance δ, ($\delta = \lambda_0/2$ and $V = V_0/2$) [23]. (In this report this factor of two was used.) It is not completely clear on whether the apparent activation volume, as defined by Ishai and used by Hawthorne, refers to a volume in which diffusion occurs in, or to an actual volume which is moving.

The values of V_0 calculated in this study, (see table 5), were determined from the data collected during the constant temperature, step-loading portion of each

specimen's creep curve. Since step-loading intervals were repeated several times for each specimen, a great deal of data could be acquired. A typical plot of the data compiled from one specimen, in this case, specimen F4, is shown in figure 9.

A check of the sum of ranks test shows that the difference between the matrix-free and composite specimens must be judged as significant. Indeed, the apparent activation volume of the carbon composite is 24% smaller than the matrix-free yarn. So even though the deformation mechanism of vacancy diffusion prevails for the two specimen types, the size of the 'volume' involved in this process is different due to the presence of the carbon matrix. It is not clear to the authors why this is so.

The two values of V_0 determined here, like the value determined by Hawthorne for his glassy carbon fibers (approximately 4000 $Å^3$), are of the same order as the apparent activation volumes found for some glassy polymers which have been subjected to high temperature deformation [13]. Hawthorne stated that this suggests that the diffusion process may operate on a molecular level and that the size of this macromolecule may be related to the size of the crystallites (the platelets of basal planes) found in the turbostratic structure of the carbon fibers.

3.8 The Work Required to Activate V_0

Equation 3 can be rewritten as

$$V_o = 4kT \frac{1}{\dot{\epsilon}} \left(\frac{d\dot{\epsilon}}{d\sigma}\right) \qquad \text{eqn. 4}$$

this includes a factor of two as suggested in Ishai's paper.

Differentiating equation 1 with respect to stress yields

$$\frac{d\dot{\epsilon}}{d\sigma} = \frac{\dot{\epsilon}n}{\sigma} \qquad \text{eqn. 5}$$

And substitution of equation 5 into equation 4 gives

$$V_o\sigma = 4kTn \qquad \text{eqn. 6}$$

where the product on the left hand side may be regarded as the work W_o needed to activate V_o.

The quantities in equation 6, as calculated from the test data, are presented in table 6. These results were derived from the constant temperature, step-loading portion of the creep tests. The stress values used for each specimen represent an average of all the stresses used during the step-loading. The values used for the stress exponent are the ones presented in table 7.

The excellent agreement of these results support the formulation of equation 6; that for a given material within a certain stress range the work and the apparent activation volume can be calculated at a given temperature. Equation 6 also implies that the apparent activation volume V_0 is linearly related to the inverse of the stress with the slope of this plot being stress exponent n dependent. Figure 10 shows this experimentally.

3.9 Stress Exponent and the Effect of Loading History

Table 7 lists the values of the stress exponent n for the matrix-free and composite specimens; there is no significant difference between the values of n for the two types of specimens. Plots of the logarithm of the strain rate versus the logarithm of the stress are compiled in figure 11 for three of the specimens. The results of other researchers, as listed by Hawthorne [13] and by Cannon [19],

show that a majority of the stress exponent values determined for graphites, fall in the 6 to 8 range. (These graphites also had activation energies in the 1000 kJ/mol range). The average value determined in this study of 7.5 compares favorably with these graphites. Obviously, creep-behavior is highly dependent on the stress.

Step-loading, whether it be in increasing or decreasing increments, had no effect on the stress dependence. This is shown be the relatively parallel lines of figure 11 - an experimental result which was observed for all the specimens.

3.10 Pre-Exponential Constant

The values of the apparent activation energy and the stress exponent, as determined for the carbon composite and matrix-free specimens, were found not to be significantly different via the sum of ranks test. Since the creep resistance of the composite specimens is much greater than that of the matrix-free specimens, when tested at the same temperature and applied load, this observed difference must manifest itself in the pre-exponential constant of equation 1.

The values of the pre-exponential constant A as calculated for the two specimen types are presented in table 8. The determination of A is dependent on the units used; the units used for the stress were 'MPa' while the units used for the steady-state strain rate were 'min^{-1}'. Because step-loading provided many values of the strain rate at different stress levels for each specimen, it was possible to calculate many values of the pre-exponential constant. Thus the results in table 8 are each specimen's average value. It was assumed that A was a constant.

The average value of A for the matrix-free specimens (12.2×10^{-3}) is larger than the average value for the composites (2.71×10^{-3}), (granted, there is a large uncertainty in these values). This order of magnitude difference is undoubtedly related to the presence of the matrix. As discussed in section 3.6, the well-bonded matrix in the composite specimens distributes the applied load more evenly amongst the carbon filaments of their test sections. It was even suggested that the matrix creates a 'sheath effect' which sets up a plastic flow inhibiting, triaxial stress state in the bonded filaments. But since the values of n and Q have been found to be the same irrespective of the matrix, the explanation for the poor creep resistance of the matrix-free specimens may simply be that only a fraction of the carbon filaments in these specimens are fully loaded at any given time during their tests. This conclusion is logical because there is no matrix to distribute loads and because of the following considerations: since the one inch gage-length is long when compared to the filaments' diameter, many of the filaments may not extend the whole length of the test section and thus may not be anchored into the matrix-reinforced ends; secondly many of the filaments may be twisted or wrinkled in the test section and thus not fully contribute to the resistance of the axially applied loads. Hence, the filaments of a matrix-free test section, which are left to support the load, creep and rupture before the rest of the filaments can lend their support. This process continues in an accelerated, sequential manner until the entire test section fails.

Some cursory calculations prove interesting here. At the same nominal stress and temperature, the steady-state strain rate of the matrix-free ('dry') specimens is greater than that of the composite specimens.

$$\dot{\varepsilon}_{dry} > \dot{\varepsilon}_{composite}$$

Now assuming that equation 1 is representative of the steady-state creep behavior of the specimens and assuming that A is a constant, since the the values of n and Q are the same for each specimen type, the pre-exponential constant must be greater for the matrix-free specimen.

$$A_{dry} > A_{composite}$$

This was shown to be true in table 8.

If only a fraction of the filaments in the matrix-free specimens actually pick up the load, then the stress experienced by these filaments will be higher than the nominal stress in the composite specimens.

$$\sigma > \sigma_{nominal} \qquad \text{(or)} \qquad \sigma = k\sigma_{nominal}$$

and therefore, $$A_{dry} = k^{n}A_{composite}$$

Where k is a constant. Using the average values from table 8 for the pre-exponential constant and setting the stress exponent equal to 7.5, one gets a value of 1.22 for k.

These calculations estimate that the true stress experienced by those matrix-free filaments that are actually loaded during creep is approximately 20% higher than the nominal stress experienced by their well-bonded counterparts. This implies that the values of n and Q obtained in this study are probably valid for much higher stress levels than those at which the composites were tested.

4. SUMMARY

In an effort to improve the understanding of the thermomechanical behavior of carbon yarn and carbon-carbon composites the following was accomplished:

Creep-behavior in uniaxial composites at high temperatures and high stresses is characterized by an initial, large transient stage followed by a steady-state response which can be modeled by a Dorn-type creep relation. The implications involved here lie with the proposal that creep be used to relieve stresses in fiber bundles during the fabrication of carbon-carbon billets. Instead of designing time-temperature processing paths on steady-state creep predictions, more of the attention should be given to the large, primary response.

The apparent activation energy for the composite and dry specimen was measured as 1082 kJ/mol (258 kcal/mol). It represents a single, thermally activated process which is the same in both specimens irrespective of the matrix. It also compares favorably with values determined by other researchers for various pyrolytic carbons, graphites, and cokes. The conclusion drawn from this comparison is that the thermally activated process is the same in all these materials for high temperature processes such as graphitization and deformation. This process is vacancy formation and motion (diffusion).

The stress state can be used to explain how the matrix improves the creep resistance of the carbon yarn. If one assumes that the matrix imposes a triaxial stress state in well-bonded yarn filaments, then the shear stress is reduced in these filaments and the flux of vacancies is therefore lessened.

Though the apparent activation energy was determined to be the same in the composite and dry uniaxial creep specimens, the apparent activation volume V_o was not. Values determined for V_o were 1583 $Å^3$ for the composite and 2088 $Å^3$ for the dry. These are of the same order as molecular scale deformation processes in some organic polymers and suggest that vacancy controlled diffusion occurs not on the atomic scale in the carbon yarn but on some 'crystallite scale'.

A quantity which represents the work needed to activate the activation volume was proposed. It can be expressed by the simple equation

$$V_o\sigma = 4kTn$$

This expression was confirmed by the data.

The stress exponent was determined to be 7.5 thus showing that the creep behavior is highly dependent on the applied load. This value serves both the dry and composite specimen and was found to be independent of the loading history.

The pre-exponential factor A was also determined. Its value was found to be 2.71×10^{-3} for the composite specimen and 12.2×10^{-3} for the matrix-free specimens. It was suggested that the difference in the creep resistance between the two specimen types may be explained simply by assuming that only a fraction of the filaments in the matrix-free specimens are fully loaded during creep. These results also suggested that the values of the stress exponent and the apparent activation energy may be valid at higher stress levels than those tested at in this study.

Combining the above results into the Dorn expression, steady-state creep in carbon yarn and carbon-carbon composites can be expressed as:

$$\ln\dot{\varepsilon} = (-6.59) + (7.49)\ln\sigma - (1082\text{kJ/mol})/RT \quad \text{(composite)}$$

$$\ln\dot{\varepsilon} = (-4.96) + (7.49)\ln\sigma - (1082\text{kJ/mol})/RT \quad \text{(dry, matrix-free)}$$

where the stress is measured in 'MPa', and the steady-state strain rate is measured in 'min^{-1}'.

REFERENCES

1. Fitzer, E., "The Future of Carbon-Carbon Composites", Carbon, 25, 163-190, (1987).

2. Mantell, C.L., Carbon and Graphite Handbook, Krieger Publishing Co., Inc., Reprint Edition, (1979).

3. Sines, G., Cohen, B.J., "Stresses During Fabrication of Cylindrically Woven Carbon-Carbon Composites", from Thermomechanical Behavior of High Temperature Composites, Edited by Jortner, J., ASME Publication AD-04, 63-76, (1982).

4. Quan, D., Sines, G., Batdorf, S.B., "The Effects of Radial Yarns - Three Dimensionally Reinforced Carbon-Carbon Composites", ONR-N0014-77-C-0505, University of California, Los Angeles, Department of Materials Science and Engineering, 89 pages, (July, 1984).

5. Evangelides, J.S., Sines, G., Batdorf, S.B., "Damage Mechanisms and Modeling of Carbon-Carbon Composites", UCLA-ENG-7975, University of California, Los Angeles, Department of Materials Science and Engineering, 73 pages, (May 1, 1981).

6. Mack, S.D., Sines, G., "High Temperature Mechanical Testing of a Cylindrical Weave Carbon-Carbon Composite", ONR-N0014-77-0505, July 1985, University of California, Los Angeles; Department of Materials Science and Engineering, 73 pages.

7. Sines, G., Yang, Z., Vickers, B.V., "Effect of the Matrix on the Creep-Behavior of Carbon-Carbon Composites", UCLA-ENG-87-44, Nov. 1987, University of California, Los Angeles, Department of Materials Science and Engineering, 29 pages.

8. Feldman, L.A., "High Temperature Creep of Carbon Yarns: Second Annual Report", Report No. TOR-0084A(5728-02)-1, The Aerospace Corporation, 85 pages, (July 15, 1985).

9. Feldman, L.A., "High Temperature Creep Effects in Carbon Yarns and Composites", Report No. TOR-0086A(2728-02)-1, The Aerospace Corporation, 12 pages, (Dec. 5, 1986).

10. Feldman, L.A., "High Temperature Creep of Carbon Yarns and Composites", Report No. TOR-0086(6728-02)-2, The Aerospace Corporation, 54 pages, (Sept. 30,1987).

11. Chauvenet, W., Spherical and Practical Astronomy, Vol.2, p,558, Lippincoff, Philadelphia, (1868).

12. Wallis, W.A., Roberts, H.V., Statistics: A New Approach, The Free Press Glencoe, Illinois, (1956).

13. Hawthorne, H.M., "The Mechanics of Stretch-Graphitization of Glassy Carbon Fibers", Journal of Material Science, 11, 97-110, (1976).

14. Poirier, J.P., Creep of Crystals, Cambridge University Press, (1985).

15. Langdon, T.G., "Activation Energy for Creep of Pyrolytic and Glassy Carbon", reprinted from Nature Physical Science, 236, No. 65, page 60 only, (March 27, 1972).

16. Lilholt, H., "Creep of Fibrous Composite Materials", Composites Science and Technology, 22, 277-294,(1985).

17. Fischbach, D.B., "The Kinetics and Mechanisms of Graphitization", Chemistry and Physics of Carbon, Vol. 7, pp. 1-105, edited by Thrower, P.A., Marcel Dekker Inc., New York, (1971).

18. Donnet, J.B., Bansal, R.C., Carbon Fibers, Marcel Dekker Inc., New York, (1984).

19. Cannon, W.R., Langdon, T.G., "Review. Creep of Ceramics. Part 1 Mechanical Characteristics", Journal of Material Science, 18, 1-50, (1983).

20. Granoff, B., "Kinetics of Graphitization of Carbon-Felt/Carbon-Matrix Composites", Carbon, 12, 405-414, (1974).

21. Dienes, G.J., "Mechanism for Self-Diffusion in Graphite", Journal of Applied Physics, 23, 1194-1200, (1952).

22. Kanter, M.A., "Diffusion of Carbon Atom in Natural Graphite Crystal", Physical Review Series 2, 107, 655-663, (1957).

23. Ishai, O., "Delayed Yielding of Epoxy Resin. II. Behavior Under Constant Stress", Journal of Applied Polymer Science, 2, 1863-1880, (1967).

TABLE 1

Carbon yarn and coal tar pitch properties as provided by the manufacturers.

HM 3000 PAN Fibers
Fabricated by Hercules Incorporated Magnamite Graphite-Fibers Division (room temperature)

Density (g/cm^3)	9.014	
Impregnated Strength (MPa)	2413	(350 ksi)
Young's Modulus, axial (GPa)	372	(54 Msi)
Young's Modulus, transverse (GPa)	10.3	(1.5 Msi)

CP277-15V coal-tar pitch
Processed by Allied Chemical Corporation

Density (g/cm^3)	1.35
Coking Value (%)	48.2
Benzene Insolubles (%)	12-18
Quinoline Insolubles (%)	4-8
Ash (%)	0.23

TABLE 2

Carbon-carbon composite creep data.
Effect of 'holding time'.

	Holding Time (min)	Steady State Strain Rate $\dot{\varepsilon}$ (in/h)	CREEP ELONGATION after 1 h.	after 6 h.
G6	5	4.39×10^{-3}	1.39×10^{-2}	3.77×10^{-2}
G7	65	3.14×10^{-3}	1.20×10^{-2}	3.13×10^{-2}

TABLE 3

Values of apparent activation energy, Q, for the composite and dry specimens.

Specimen	Constant Stress σ (MPa)	Temp. Range T (°C)	App. Activation Energy Q (kJ/mol)
Composite			
G1	724	2150-2265	1016
G2	600	2150-2220	1112
G3	800	2120-2300	1225
G4	827	2170-2300	1055
			1110 ±92 (avg.)
Matrix-Free			
F1	455	2150-2430	1241
F4	538	2250-2400	990
F5	572	2120-2300	1028
F6	648	2250-2370	1043
F7	607	2120-2280	1025
			1058 ±84 (avg.)
			1082 ±92 (avg.)

TABLE 4

Theoretical activation energies for carbon atoms in graphite as calculated by Dienes [ref. 29, 1952] and later by Kanter [ref. 30, 1957].

Process	Energy (kJ/mol)	
	Dienes	Kanter
Formation of Vacancy	500	711
Motion of Vacancy	299	389
Totat Energy for Diffusion by Vacancy Mechanism	799	1100
Direct Interchange	378	473
Interstitial Mechanism	1745	1955

TABLE 5

Apparent activation volume.

Specimen	$\frac{\Delta \ln \dot{\varepsilon}}{\Delta\sigma}$ (avg.) (1/ksi)	App. Activation Volume V_o ($Å^3$)
Composite		
G1	0.0794	1640
G2	0.0909	1878
G3	0.0778	1608
G4	0.0584	1208
		1583 (avg.)
Matrix-Free		
F1	0.1224	2529
F4	0.0998	2062
F5	0.1048	2166
F6	0.0907	1874
F7	0.0875	1808
		2088 (avg.)

$V_o = 4kT\left(\frac{\Delta \ln \dot{\varepsilon}}{\Delta\sigma}\right)$ at constant temperature.

Temp. = 2310 °C (2583 °K) for all data.

TABLE 6

Work requried to activat V_o.
See equation 6.

Specimen	$\bar{\sigma}$ (MPa)	$V_o\bar{\sigma}$ $(=W_o)$ $(Jx10^{-19})$	4kTn $(Jx10^{-19})$	
Composite				
G1	671	11.01	11.13	
G2	603	11.34	10.59	
G3	705	11.35	11.40	
G4	858	10.38	10.90	
		11.02±0.45	11.01±0.34	(avg.)
Matrix-Free				
F1	394	9.98	9.88	
F4	465	9.60	9.27	
F5	523	11.34	10.84	
F6	656	12.31	12.40	
F7	556	10.05	10.12	
		10.62±1.06	10.50±1.20	(avg.)
		10.82±0.87	10.73±0.91	(avg.)
		10.77±0.87	(avg. of all data)	

T=2310 °C

n values are found in table 8

$\bar{\sigma} = 1/N(\sigma_1+\sigma_2+ \ldots\sigma_N)$

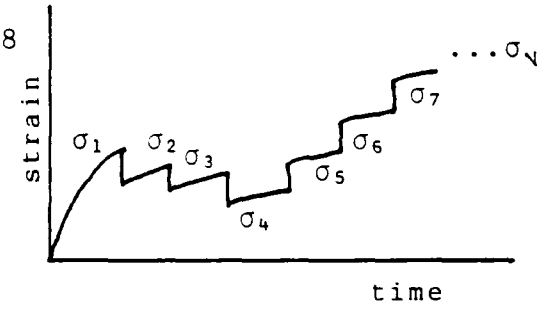

TABLE 7

The stress exponent n.

Specimen	Const. Temp. T (°C)	Stress Range σ_o (MPa)	n
Composite			
G1	2310	462-770	7.81
G2	2310	424-770	7.43
G3	2310	539-809	8.00
G4	2310	693-1002	7.15
			7.60 ±0.40
Matrix-Free			
F1	2310	308-424	6.93
F4	2310	385-501	6.50
F5	2310	424-559	7.61
F6	2310	539-732	8.70
F7	2310	424-616	7.06
			7.36 ±0.84
			7.47 ±0.66

TABLE 8

Values of the pre-exponential constant A.

Composite Specimen	G1	G2	G3	G4
ln A (avg)	-6.14	-4.89	-6.95	-8.39
	-6.594 ± 1.47			
A (x 10^{-3})	2.15	7.52	0.96	0.23
	2.71 ± 3.3			

Matrix-Free Specimen	F1	F4	F5	F6	F7
ln A (avg)	-3.37	-4.36	-4.92	-6.94	-5.21
	-4.96 ± 1.31				
A (x 10^{-3})	34.4	12.8	7.3	0.97	5.46
	12.2 ± 13.0				

The pre-exponential constant was calculated using the following expression:

$$\ln A = \ln \varepsilon - \bar{n}(\ln \sigma) + \bar{Q}/RT$$

Where the steady-state strain rate and the stress (corrected for strain) were measured form the step-loading portion of each specimen's creep test.

The units used were: $\dot{\varepsilon}$ [min^{-1}]

σ [MPa]

The other constants used were as follows:

		$\bar{n}$	$\bar{Q}$ (cal/mol)	R (cal/mol °K)	T (°K)
Composite Specimens,	G	7.599	263,200	1.987	2583
Matrix-Free Specimens,	F	7.360	252,740	1.987	2583

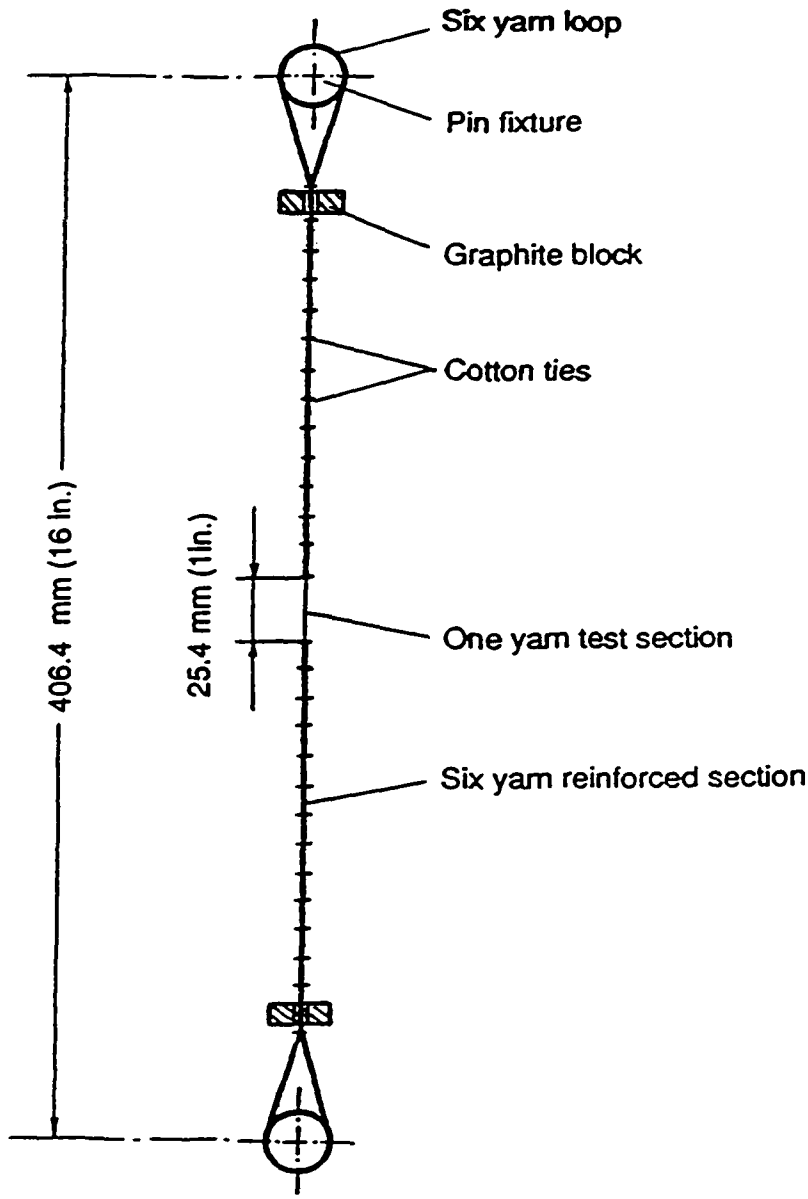

Fig. 1. Diagram of a uniaxial creep specimen. A single carbon yarn makes up the test section and extends the length of the specimen.

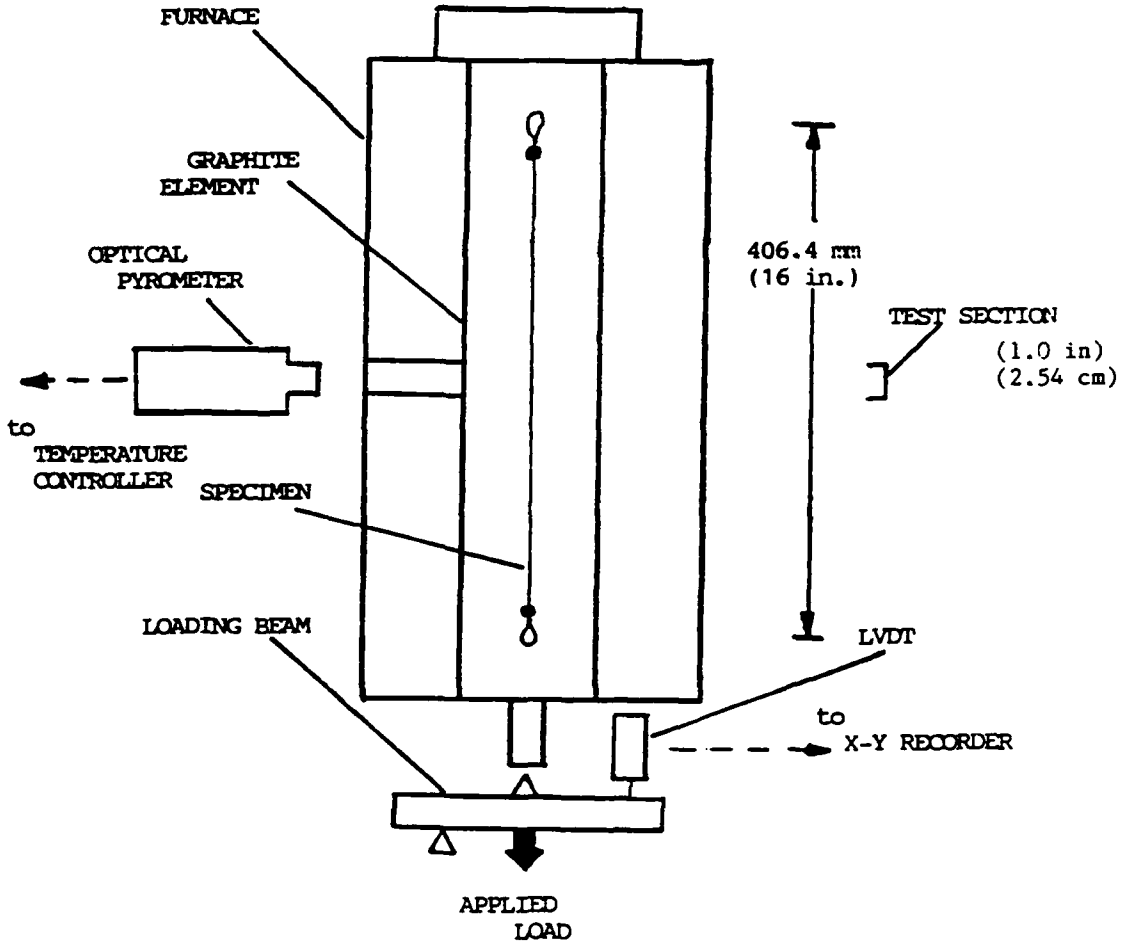

Fig. 2. Schematic of the testing apparatus. See figure 3 for a detailed drawing of the furnace arrangement.

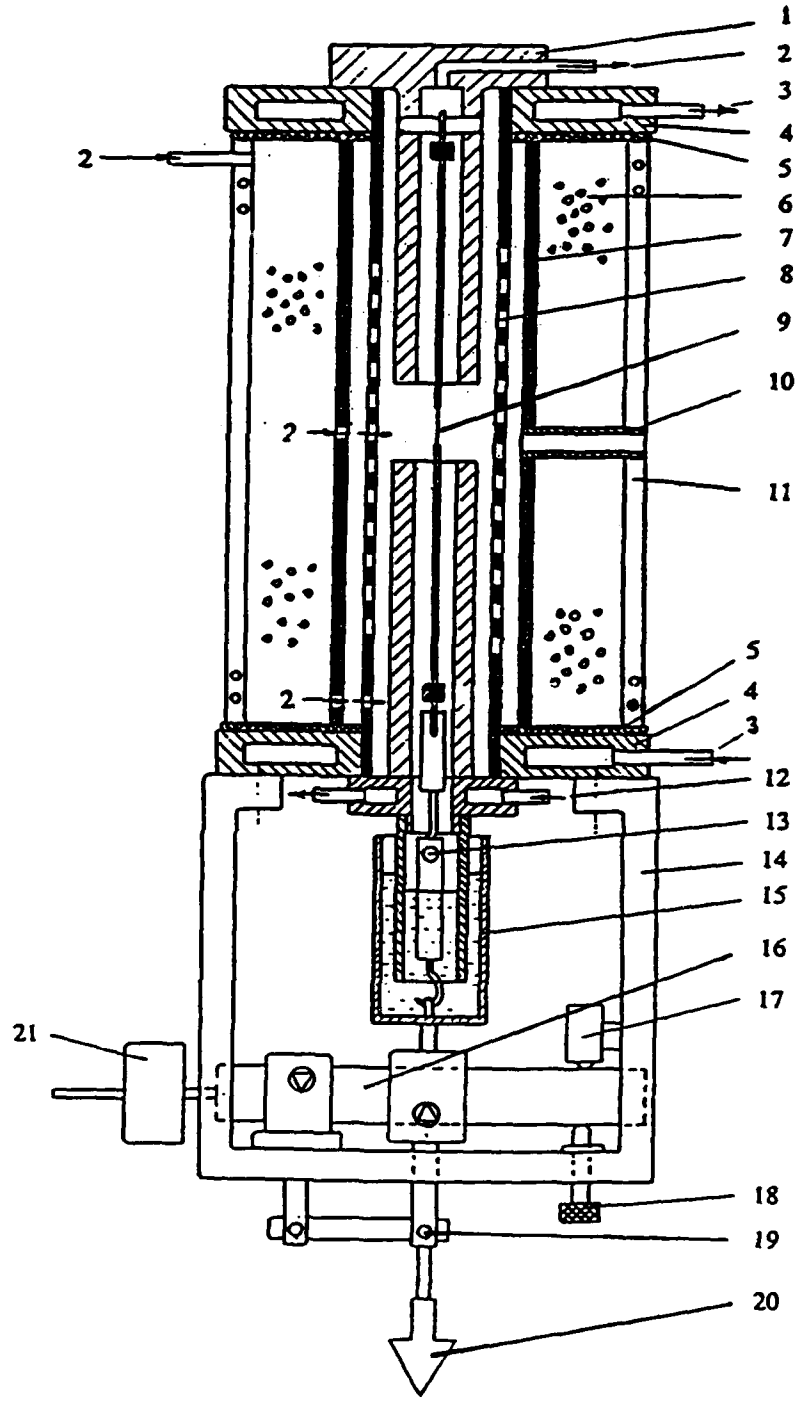

Fig. 3. Diagram of the high temperature furnace and the loading apparatus used for the creep experiments. (See the following page for number identification.)

1. Upper graphite test fixture (with pin to support test specimen)
2. Helium Inlets/outlet
3. Water Coolant Inlet/Outlet and Electrical Power Terminal
4. Upper/Lower Bulkhead Assembly
5. Electrical Insulator
6. Graphite Felt Pad Thermal Insulation
7. Graphite Shield
8. Graphite Heating Element
9. Uniaxial Creep Specimen
10. Window for Optical Pyrometer
11. Outer Furance Shell (water cooled by internal piping)
12. Lower Water Cooled Jacket
13. Specimen-Rotating Beam Linkage (including universal joint)
14. Loading Frame
15. Water Seal
16. Loading Beam
17. LVDT
18. Screw Support
19. Guide Link
20. Dead Weight Load
21. Counter Balance

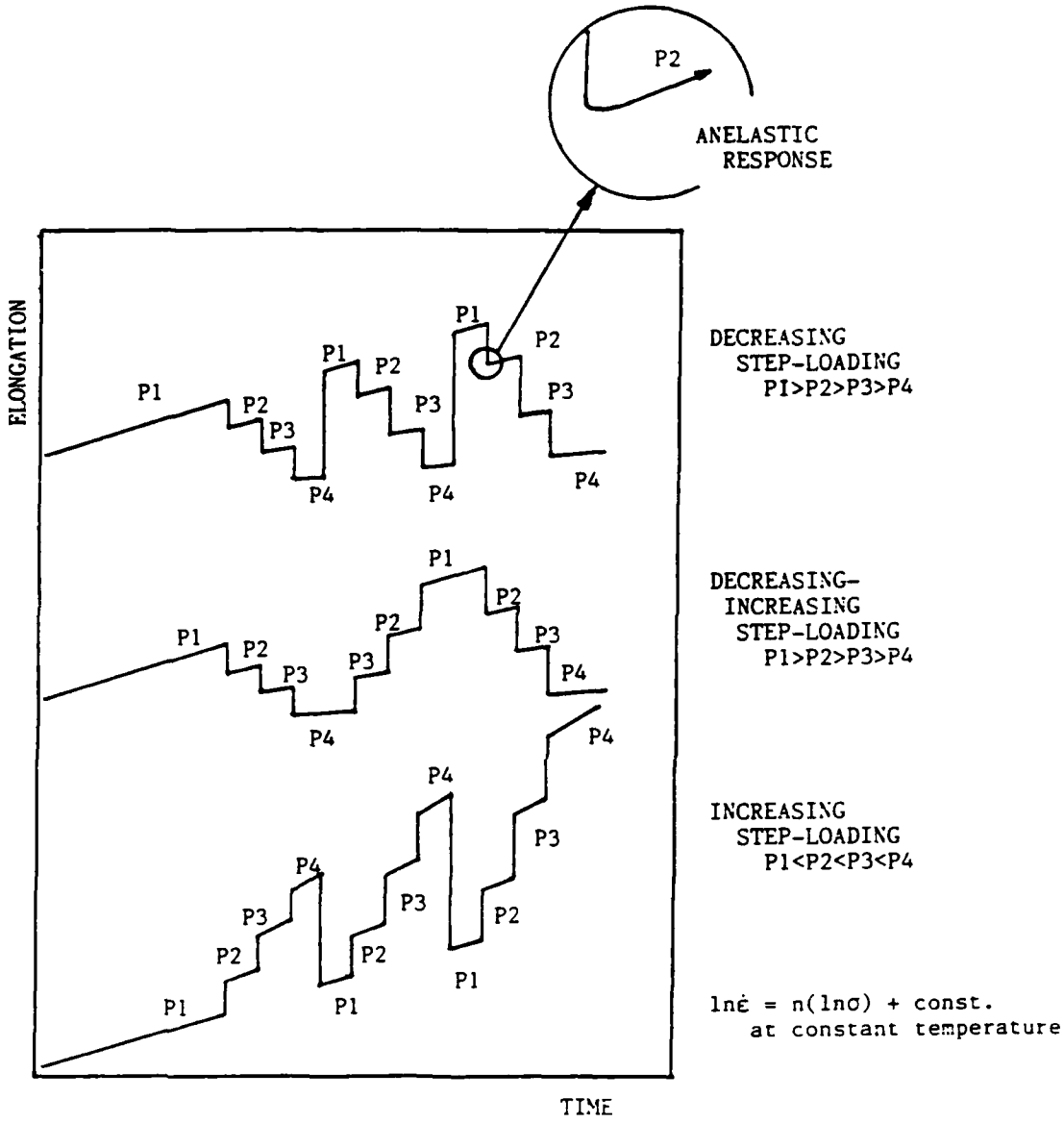

Fig. 4. A schematic showing the different procedures used to apply the load P during the constant temperature portion of the creep tests are illustrated here. When loads were decreased, a momentary, (1 to 5 mins.), anelastic response would be recorded before the linear, steady state resumed.

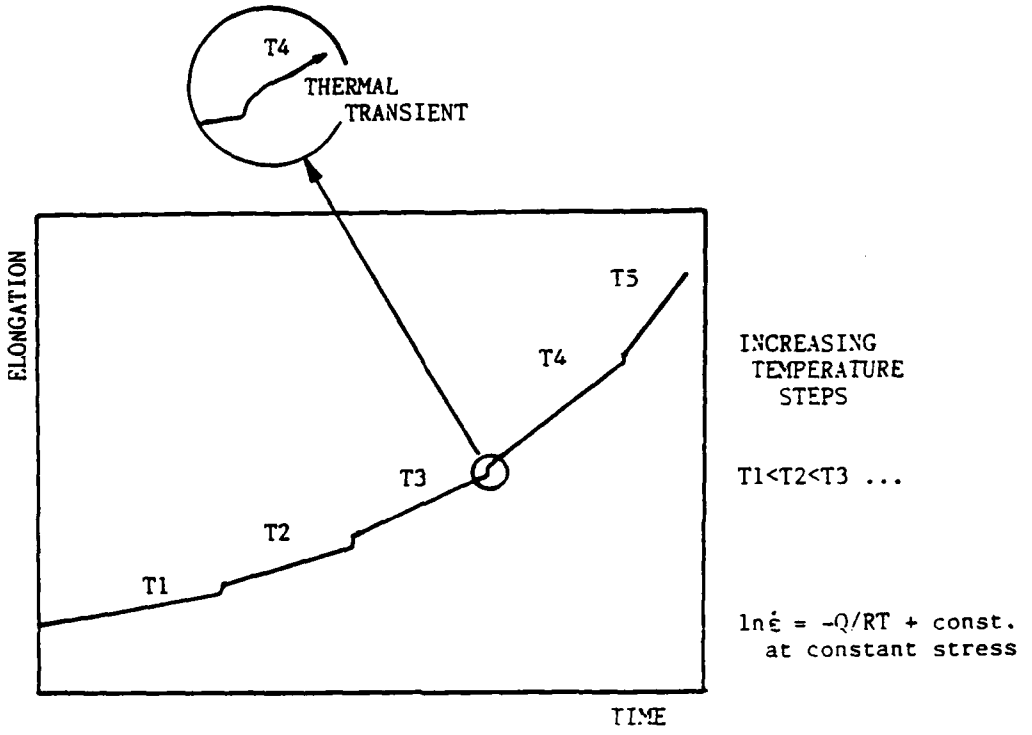

Fig. 5. Increasing temperature steps during a constant applied load were used to determine the apparent activation energy Q. The thermal transient represents the thermal response of the specimen and testing apparatus to a sudden temperature change.

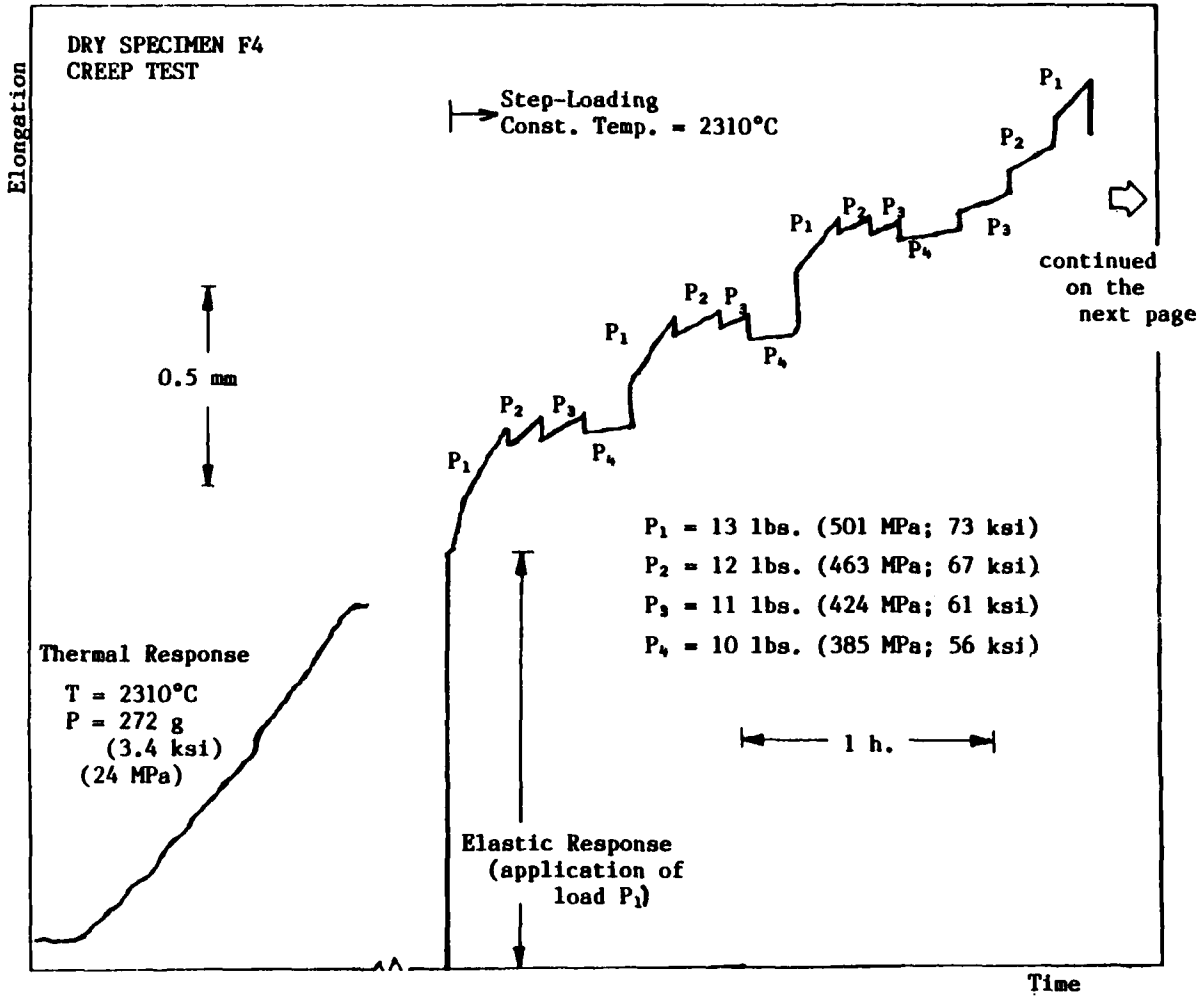

Fig. 6. The creep test of dry specimen F4. This figure is a scaled reproduction of the recordings taken from the actual test. (continued on the following page.)

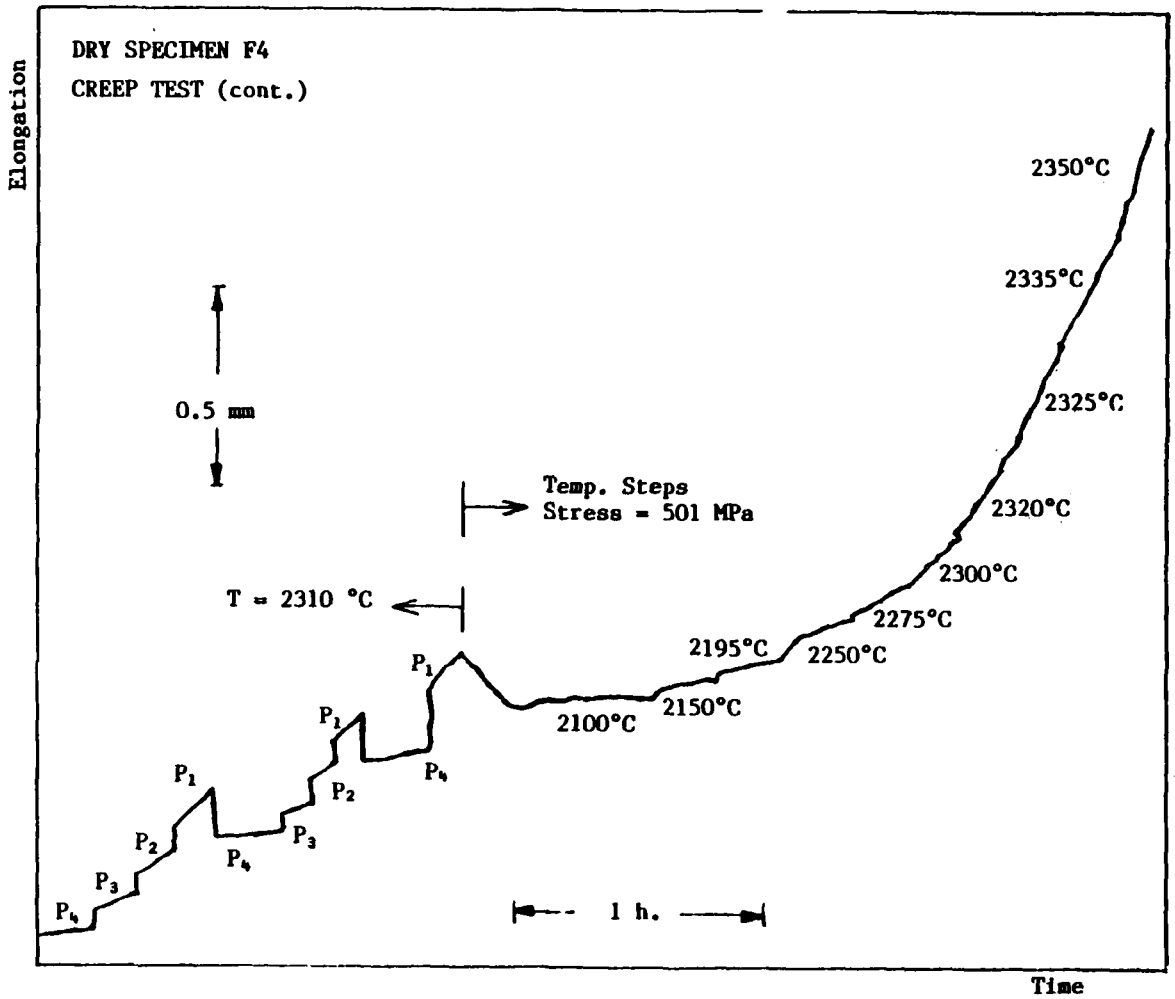
DRY SPECIMEN F4
CREEP TEST (cont.)
Elongation
0.5 mm
Temp. Steps
Stress = 501 MPa
T = 2310 °C
2350°C
2335°C
2325°C
2320°C
2300°C
2275°C
2250°C
2195°C
2150°C
2100°C
P1
P2
P3
P4
1 h.
Time

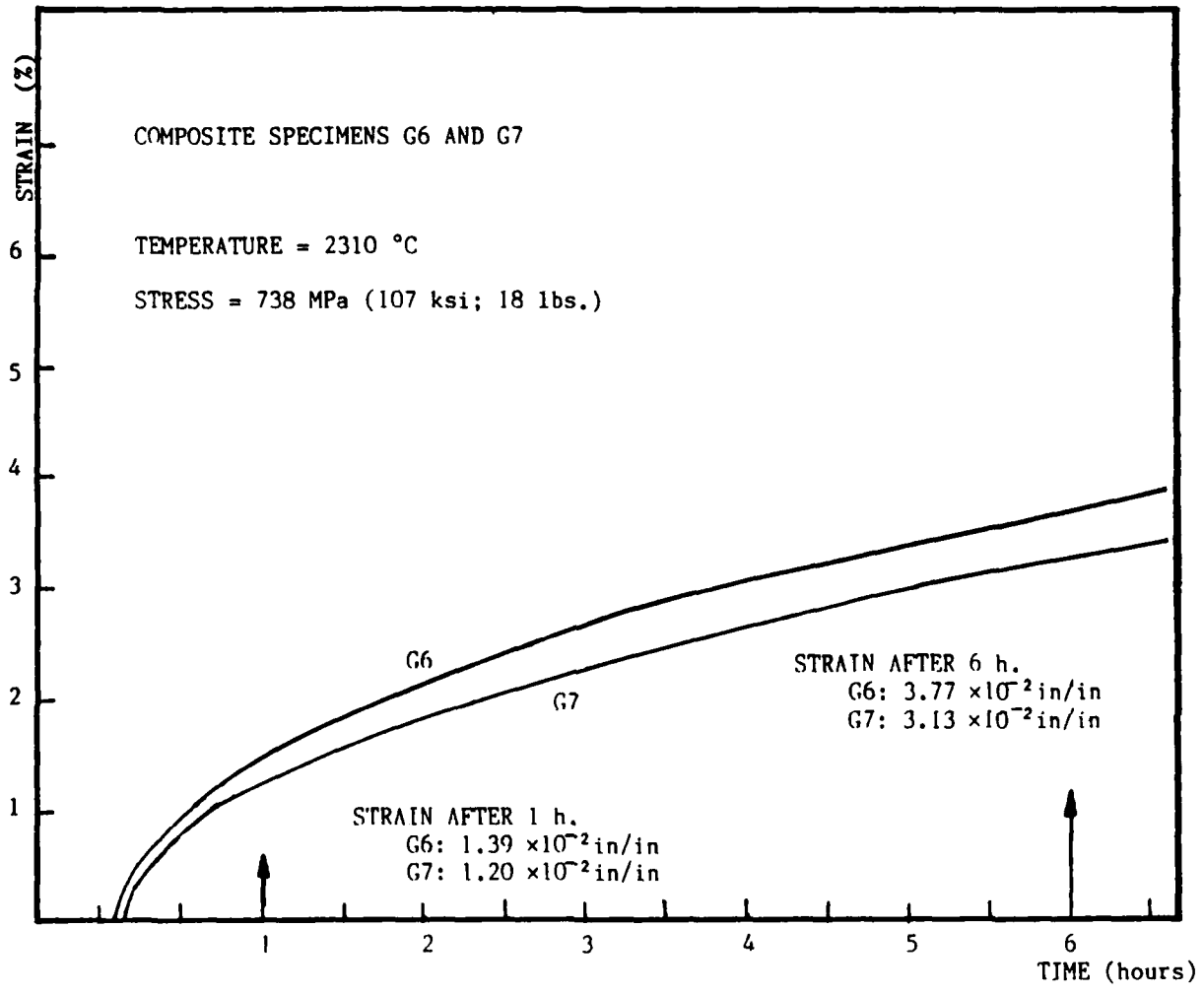

Fig. 7. Scaled reproductions of the creep curves of matrix-free ('dry') specimens G6 and G7. (See table 2.)

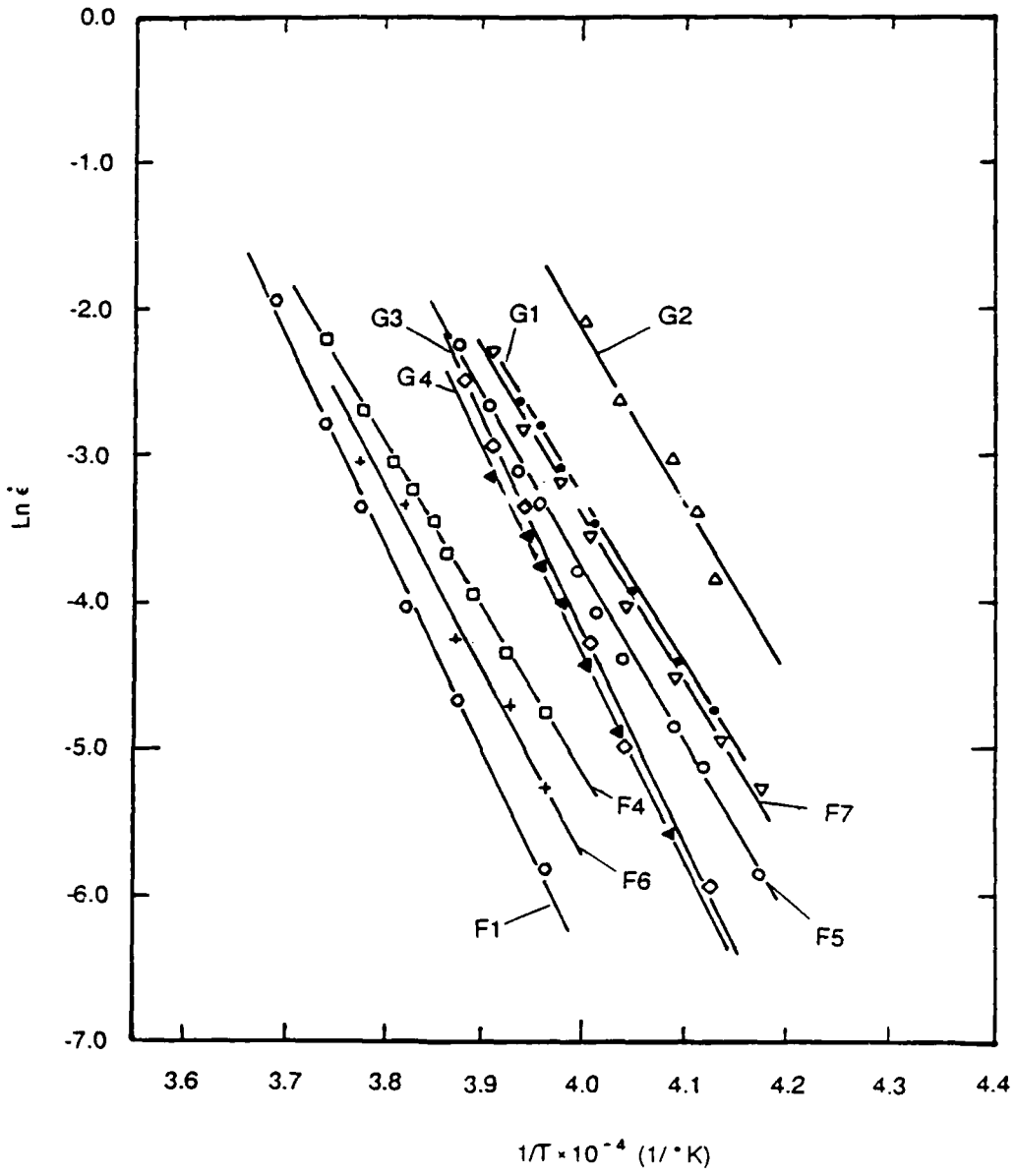

Fig. 8. The Arrhenius plots of all nine specimens used in the determination of the apparent activation energy Q. (See table 3.)

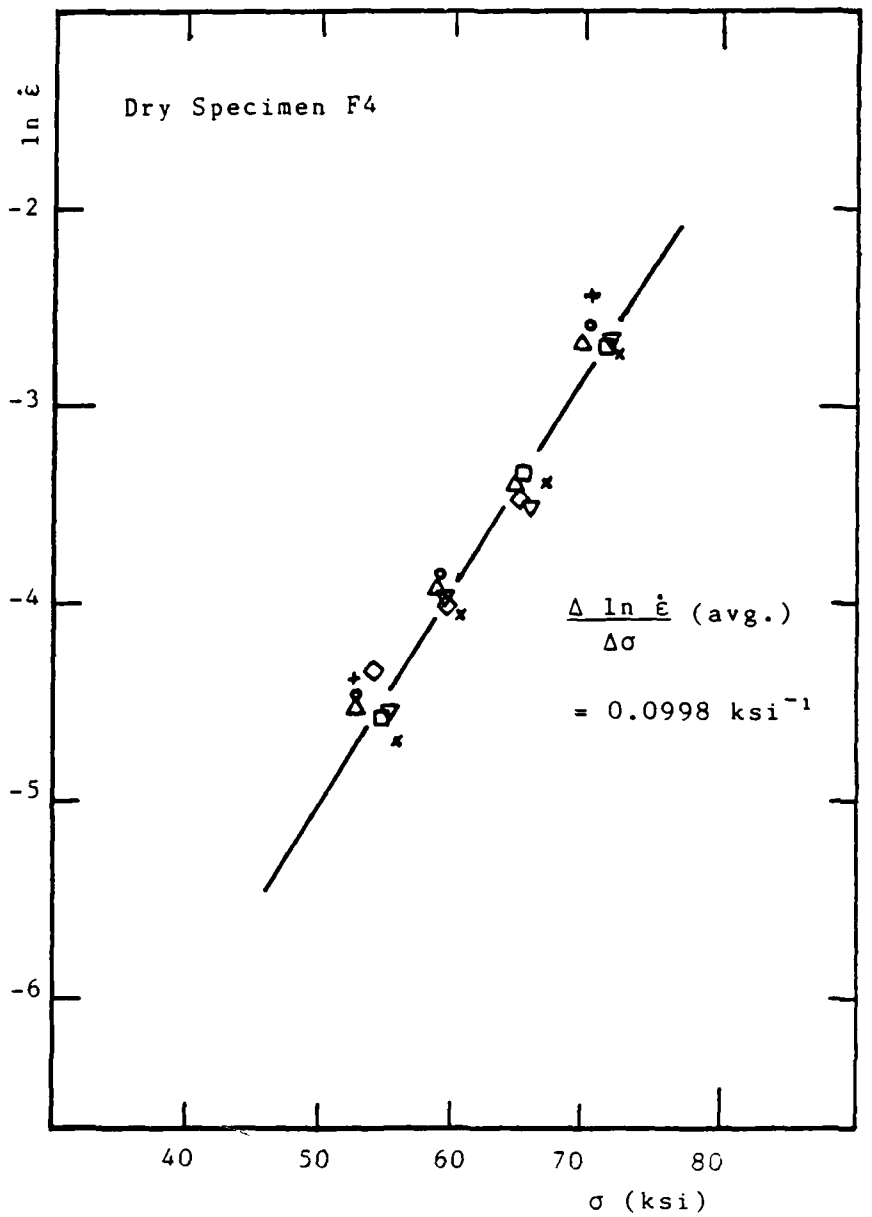

Fig. 9. Data plotted from the step-loading portion of specimen F4's creep test, used in the determination of the apparent activation volume. (See table 5.) The different plotted symbols refer to the direction of loading. See the caption of figure 11 for a detailed explanation.

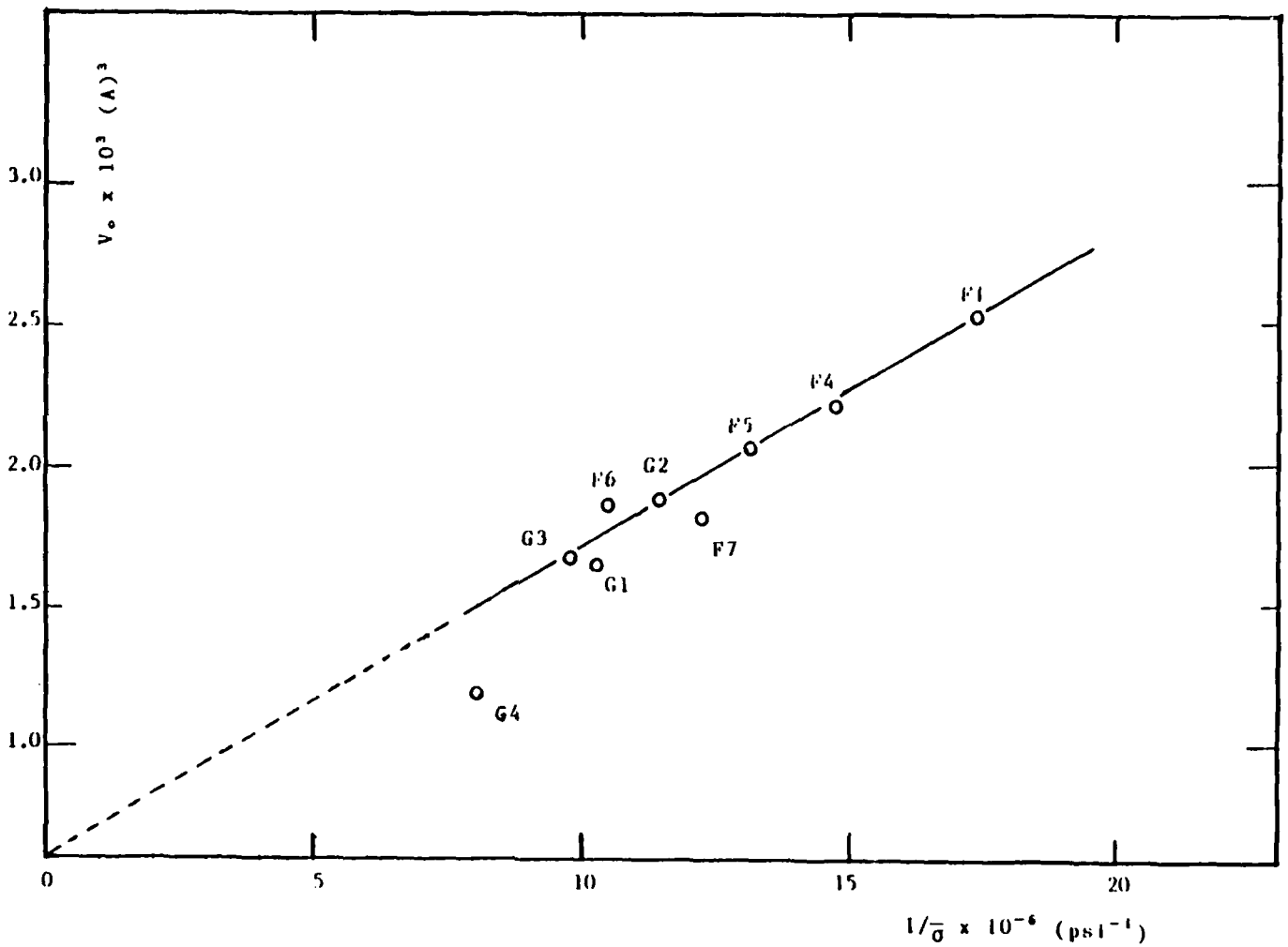

Fig. 10. Plot of the apparent activation volume V_o as a function of the inverse applied stress for the matrix-free and composite carbon specimens. (See equation 6.)

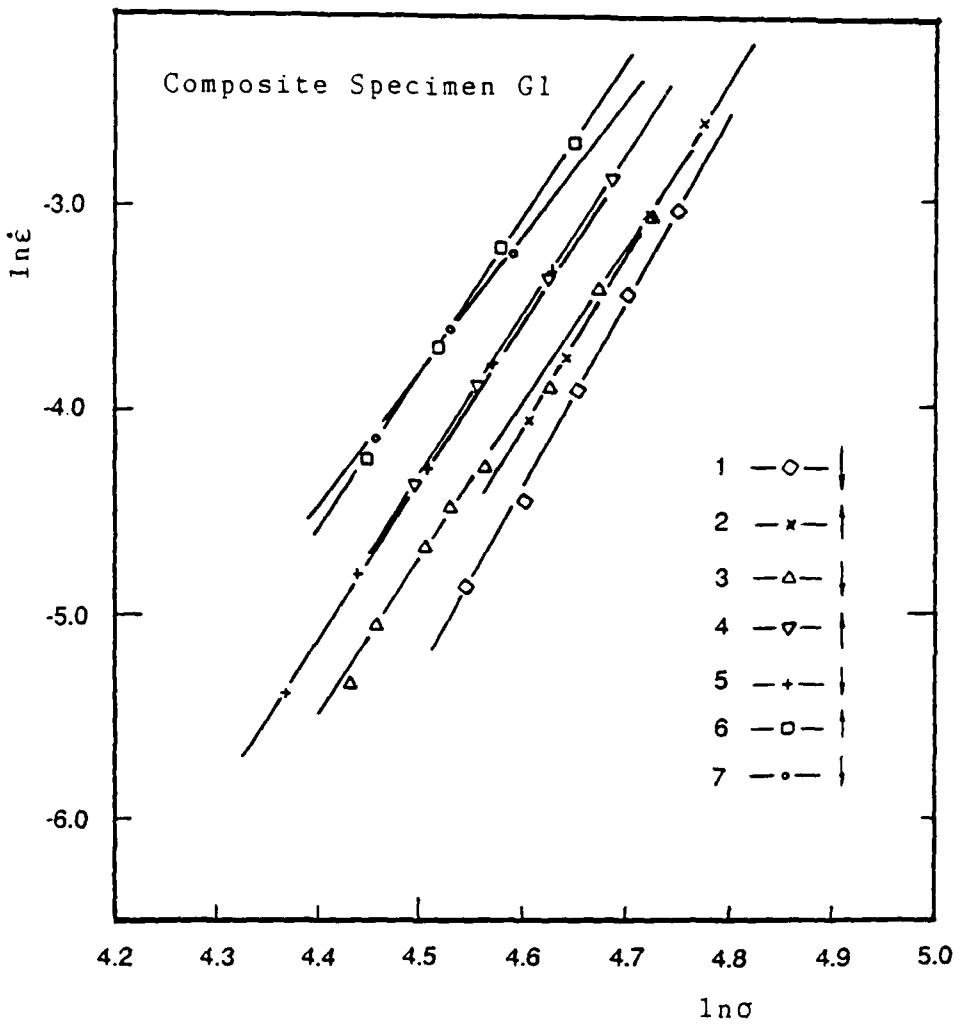

Fig. 11. The data plotted for three specimens, (composite specimen G1 on this page and matrix-free ('dry') specimens F4 and F7 on the two subsequent pages) used in the determination of the stress exponent n are shown.

Each specimen went through several 'steps' of increasing and decreasing loads, (see figure 11.). As an example, composite specimen G1 on this page went through 7 'steps' which allowed for 7 sets of data to be plotted. The value of n was then determined from all the values calculated from the slopes of the 7 plots.

The downward pointing arrows signify decreasing load steps. Upward pointing arrows signify increasing load steps. Similar plots were obtained for all of the specimens. The parallel appearance of each set of plots indicates that the loading history has no effect on subsequent creep-behavior (within reasonable stress ranges).

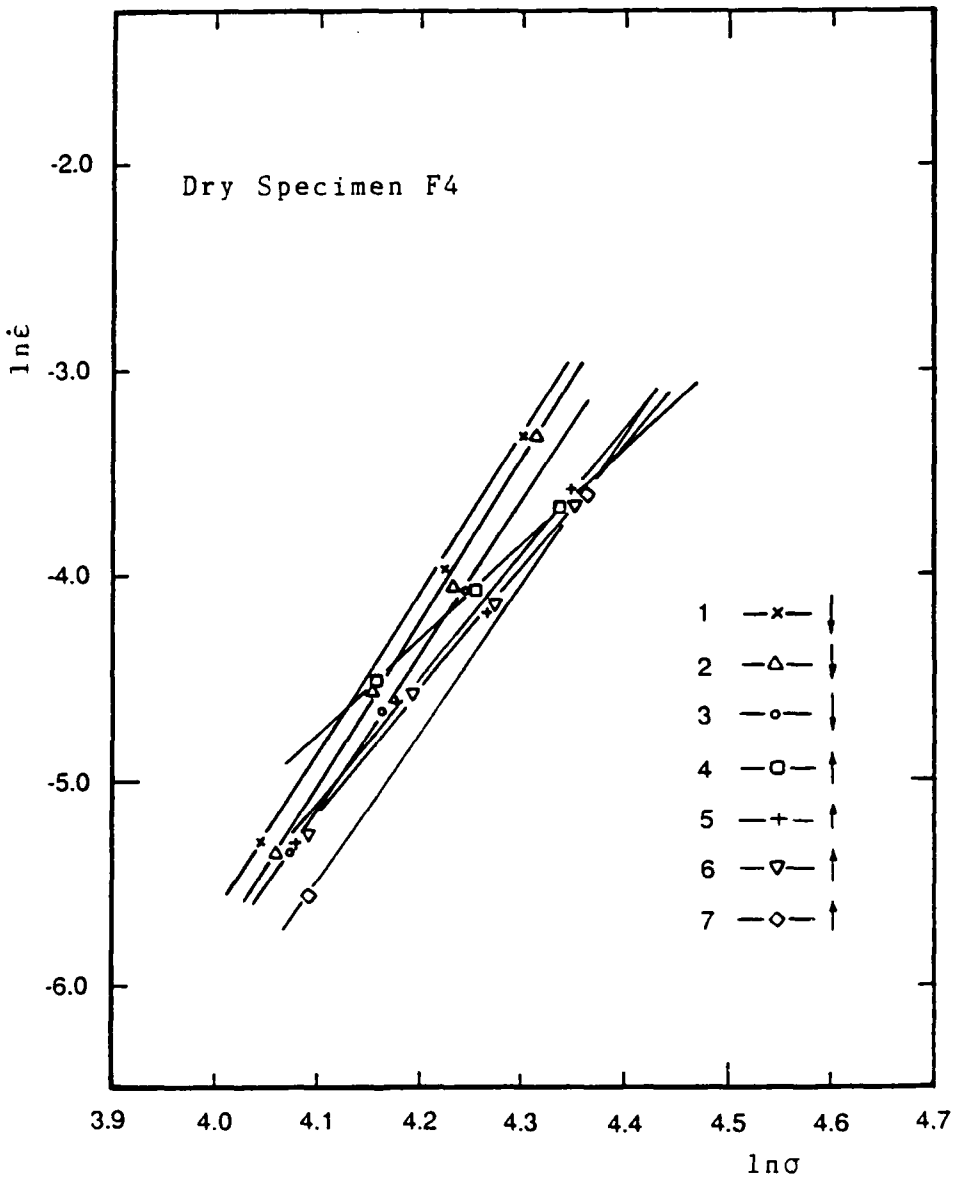
Dry Specimen F4
-2.0
-3.0
-4.0
-5.0
-6.0
lnε̇
3.9
4.0
4.1
4.2
4.3
4.4
4.5
4.6
4.7
lnσ
1
2
3
4
5
6
7

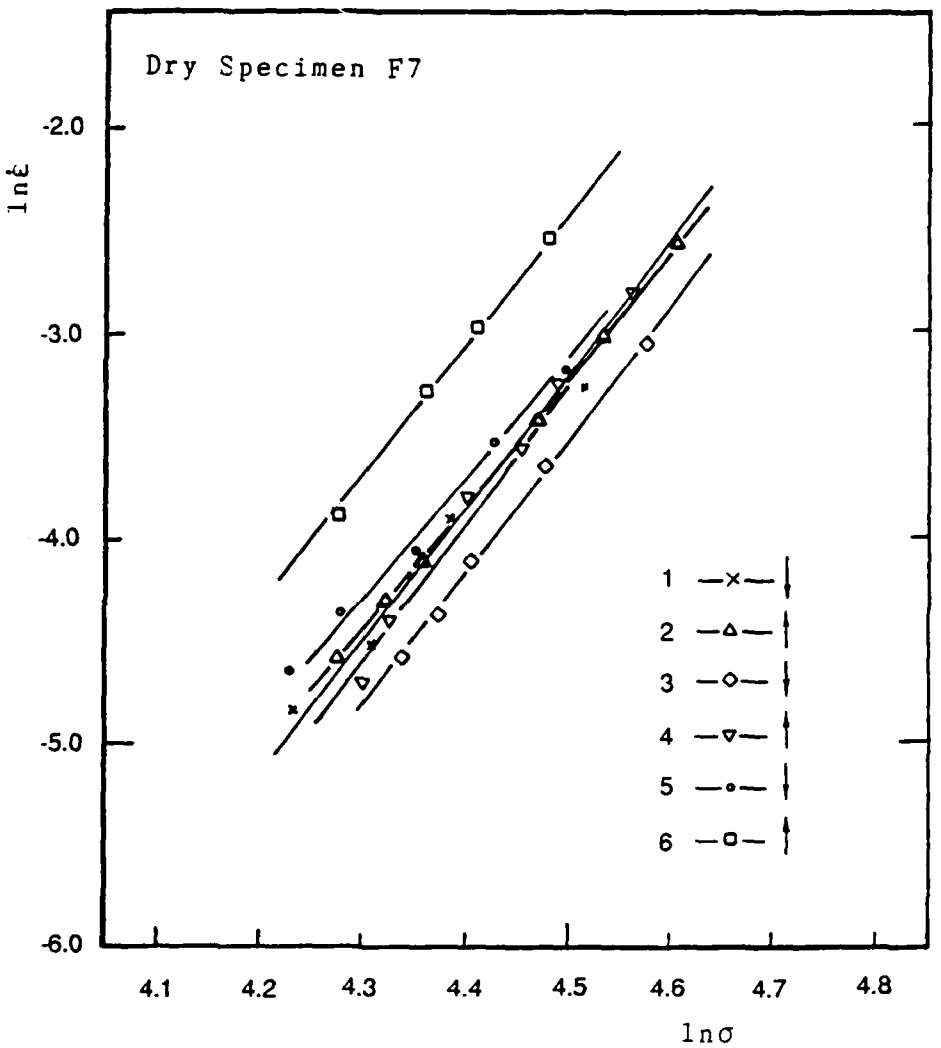
Dry Specimen F7
-2.0
-3.0
-4.0
-5.0
-6.0
lnε̇
4.1
4.2
4.3
4.4
4.5
4.6
4.7
4.8
lnσ
1
2
3
4
5
6

ORGANIZATION	LASTNAME	FIRSTNAME	CITY	STATE	ZIPCODE
	Batdorf	S. B.	Laguna Hills	CA	92653
	White	J. L.	Del Mar	CA	92014
ACUREX/AEROTHERM	Carlson	D. L.	Mountain View	CA	94039
ACUREX/AEROTHERM	Zimmer	J. E.	Mountain View	CA	94039
AEROJET STRATEGIC PROPULSION CO	Suhoza	Jim	Sacramento	CA	95813
AEROJET STRATEGIC PROPULSION COMPANY	Payne	William	Sacramento	CA	95813
AEROSPACE CORPORATION	Feldman	L.	Los Angeles	CA	90009
AEROSPACE CORPORATION	Katzman	Howard	Los Angeles	CA	90009
AEROSPACE CORPORATION	Meyer	Robert A.	Los Angeles	CA	90009
AEROSPACE CORPORATION	Rellick	G. S.	Los Angeles	CA	90009
AFOSR/NC	Ulrich	D. R.	Bolling AFB	DC	20332
AFWAL/ML	Librarian		Wright-Patterson AFB	OH	45433
AFWAL/MLBC	Abrams	Frances	Wright-Patterson AFB	OH	45433
AFWAL/MLBC	Schmidt	D.	Wright-Patterson AFB	OH	45433
AFWAL/MLBC	Theibert	L. Scott	Wright-Patterson AFB	OH	45433
AFWAL/MLBE	Craig	R. E.	Wright-Patterson AFB	OH	45433
AFWAL/MLBM	Pagano	N. J.	Wright-Patterson AFB	OH	45433
AFWAL/MLLM	Kerans	R.	Wright-Patterson AFB	OH	45433
AIR FORCE ASTRONAUTICS LAB	Hildreth	J.	Edwards AFB	CA	93523
AIR FORCE ASTRONAUTICS LAB	Ismail	I.	Edwards AFB	CA	93523
AIR FORCE ASTRONAUTICS LAB	Pollock	Peter	Edwards AFB	CA	93523
AIR FORCE ASTRONAUTICS LAB	Tepe	L.	Edwards AFB	CA	93523
AMMRC	Uhlir	Donald A.	Watertown	MA	02172
AMOCO PERFORMANCE PRODUCTS, INC.	Bacon	Roger	Parma	OH	44130
ARMY MATERIALS & MECHANICS RES. CENTER	Dignam	J.	Watertown	MA	02172
ARMY RESEARCH OFFICE	Meyer	George	Research Triangle Pk	NC	27709
ASHLAND PETROLEUM CO	Newman	John W.	Ashland	KY	41114
ATLANTIC RESEARCH CORPORATION	Baetz	J.	Alexandria	VA	22314
AVCO Corporation	Laskaris	T.	Lowell	MA	01851
AVCO Corporation	Rolincik	P.	Wilmington	MA	01887
AVCO Systems Division	Taverna	Art	Wilmington	MA	01887
B.F. GOODRICH R&D CENTER	Price	R. J.	Brecksville	OH	44191
B.F. GOODRICH R&D CENTER	Stover	E.	Brecksville	OH	44191
B.F.GOODRICH-SUPERTEMP CENTER	Engle	Glen B.	Santa Fe Springs	CA	90670
BATTELLE COLUMBUS LABORATORIES	Jelinek	Frank J.	Columbus	Ohio	43201
BOEING AEROSPACE CO	Nelson	James M.	Seattle	WA	98124
CALIFORNIA RESEARCH & TECHNOLOGY, INC.	Krevenhagen	K. N.	Chatsworth	CA	91311
CASE WESTERN RESERVE UNIVERSITY	Moet	A.	Cleveland	OH	44106
DARPA	Patten	F.	Arlington	VA	22209
DCASMA-Santa Ana	Crowe	L. L.	Santa Ana	CA	92712-2700
DEFENSE NUCLEAR AGENCY	Kohler	D.	Washington	DC	20305
DEFENSE TECHNICAL INFORMATION CENTER	**********		Alexandria	VA 22314	22314
DOW CORNING CORPORATION	Hauth	W. E.	Midland	MI	48640
EFFECTS TECHNOLOGY, INC.	Adler	W.	Santa Barbara	CA	93105
EHRENPREIS CONSULTING ENGINEERS	Ehrenpreis	David	Fort Lee	NJ	07024
EXXON ENTERPRISES, INC.	Riggs	D.	Fountain Inn	SC	29644
FAILURE ANALYSIS ASSOCIATES	Frankle	Robert	Palo Alto	CA	94303
FIBER MATERIALS, INC.	Burns	Robert L.	Biddeford	ME	04005
FIBER MATERIALS, INC.	Lander	L. L.	Biddeford	ME	04005

ORGANIZATION	LASTNAME	FIRSTNAME	CITY	STATE	ZIPCODE
GA Technologies	Sheehan	James	San Diego	CA	92138
GENERAL DYNAMICS	Uhl	David	Ft. Worth	TX	76101
GENERAL DYNAMICS - FORT WORTH DIV	Henson	Michael	Ft. Worth	TX	76101
GENERAL DYNAMICS CONVAIR	McNamara	Raymond	San Diego	CA	92138
GENERAL ELECTRIC COMPANY	Franke	Robert	Cincinnati	OH	45215
GENERAL ELECTRIC COMPANY	Hall	Kenneth J.	Philadelphia	PA	19101
GEORGIA INSTITUTE OF TECHNOLOGY	Abhiraman	A. S.	Atlanta	GA	30332
HERCULES CORPORATION	Christensen	P.	Magna	UT	84044
HITCO	Dyson	L.	Gardena	CA	90249
HITCO	Fordham	Paul A.	Gardena	CA	90249
IIT Research Institute	Larsen	D. C.	Chicago	Illinois	60616
INSTITUTE FOR DEFENSE ANALYSIS	Kearns	T. F.	Alexandria	VA	22311
JET PROPULSION LABORATORY	Librarian		Pasadena	CA	91103
JORTNER RESEARCH & ENGINEERING, INC.	Jortner	Julius	Costa Mesa	CA	92628
KAISER	Fischer	M.	San Leandro	CA	94577
KAISER AEROTECH	Davis	H. G.	San Leandro	CA	94577
LAWRENCE LIVERMORE LABORATORIES	Maimoni	A.	Livermore	CA	94550
LOCKHEED MISSILES & SPACE CO, INC	Weiler	Frank	Palo Alto	CA	94304-1191
LOCKHEED MISSILES & SPACE COMPANY, INC.	Pinoli	Pat C.	Palo Alto	CA	94304
LOCKHEED MISSILES AND SPACE COMPANY	Osaka	W.	Sunnyvale	CA	94088
LOCKHEED PALO ALTO RESEARCH LAB	Crossman	Frank	PAlo Alt	CA	94304
LOS ALAMOS SCIENTIFIC LABORATORY	Riley	R. E.	Los Alamos	NM	76545
MARTIN MARIETTA AEROSPACE	Koo	F. H.	Orlando	FL	32855
MATERIALS SCIENCES CORPORATION	Kibler	J. J.	Springhouse	PA	19477
MATERIALS SCIENCES CORPORATION	Rosen	B. Walter	Springhouse	PA	19477
MCDONNELL DOUGLAS ASTRONAUTICS CO.	Greszczuk	L. B.	Huntington Beach	CA	92647
MCDONNELL DOUGLAS ASTRONAUTICS CO.	Penton	A. P.	Huntington Beach	CA	92647
MCDONNELL DOUGLAS RESEARCH LABORATORY	Holman	H.	St. Louis	MO	63166
NADC	Barker	William	Warminster	PA	18974
NASA Langley	Houston	R. J.	Langley	VA	23665
NASA Langley	Maahs	Howard	Langley	VA	23665
NASA Langley	Rummler	D.	Langley	VA	23665
NASA LANGLEY RESEARCH CTR	Library		Langley Field	VA	23365
NASA Marshall Space Flight Center	Nowakowski	Michael	Huntsville	AL	35812
NASA Marshall Space Flight Center	Powers	B.	Huntsville	AL	35812
NASA MARSHALL SPACE FLIGHT CTR	Library		Huntsville	AL	35812
NAVAL RESEARCH LABORATORY	Badaliance	Robert	Washington	DC	20375
NAVAL RESEARCH LABORATORY	Director		Washington	DC	20375
NAVAL SEA SYSTEMS COMMAND	Kinna	M.	Washington	DC	20302
NAVAL WEAPONS CENTER	Schwartz	Robert	China Lake	CA	93555
NSWC/WOL	Edwards	R. J.	Silver Spring	MD	20910
NSWC/WOL	Rowe	Charles R.	Silver Spring	MD	20910
NSWC/WOL	Thompson	J.	Silver Spring	MD	20910
OFFICE OF NAVAL RESEARCH	**********		Pasadena	CA	91106
OFFICE OF NAVAL RESEARCH	Diness	A. M.	Arlington	VA	22217
OFFICE OF NAVAL RESEARCH	Kushner	A. S.	Arlington	VA	22217
OFFICE OF NAVAL RESEARCH	Peebles	L. H.	Arlington	VA	22217
OFFICE OF NAVAL RESEARCH	Pohanka	Robert	Arlington	VA	22217
OSD/DDR&E	Persh	J.	Washington	DC	20301

ORGANIZATION	LASTNAME	FIRSTNAME	CITY	STATE	ZIPCODE
PDA Engineering	Crose	J. G.	Santa Ana	CA	92705
PDA Engineering	Stanton	E. L.	Santa Ana	CA	92705
PENNSYLVANIA STATE UNIVERSITY	Thrower	P. A.	University Park	PA	16802
PRATT & WHITNEY AIRCRAFT	Schmid	Tom	West Palm Beach	FL	33402
PURDUE UNIVERSITY	Sun	C. T.	West Lafayette	IN	47907
RENSSELAER POLYTECHNIC INSTITUTE	Diefendorf	R. J.	Troy	NY	12181
ROCKWELL INT'L SCIENCE CENTER	Muir	Art	Thousand Oaks	CA	91360
SANDIA LABORATORIES	Northrup	D.	Albuquerque	NM	87185
SCIENCE APPLICATIONS INT'L CORPORATION	Clayton	F. I.	Irvine	CA	92715
SCIENCE APPLICATIONS INT'L CORPORATION	Loomis	Willard	Irvine	CA	92715
SOUTHERN ILLINOIS UNIVERSITY	Wright	Maurice	Carbondale	IL	62901-4303
SOUTHERN RESEARCH INSTITUTE	Koenig	John	Birmingham	AL	35205
SOUTHERN RESEARCH INSTITUTE	Pears	C.	Birmingham	AL	35205
SOUTHERN RESEARCH INSTITUTE	Starrett	H. Stuart	Birmingham	AL	35205
STACKPOLE FIBERS COMPANY, INC.	Fleming	G.	Lowell	MA	01852
STRATEGIC SYSTEMS PROJECT OFFICE (PM-1)	Commander		Washington	DC	20376
SYSTEMS, SCIENCE AND SOFTWARE	Gurtman	G.	La Jolla	CA	92037
THIOKOL	Broman	G.	Brigham City	UT	84302
TRW Systems	Kotlensky	Wm.	San Bernardino	CA	92402
UNION CARBIDE CORPORATION	Bowman	J.	Cleveland	OH	44101
UNION CARBIDE CORPORATION	Library		Oak Ridge	TN	37839
UNITED TECHNOLOGIES RESEARCH CENTER	Gallaso	F.	Hartford	CT	06100
UNITED TECHNOLOGIES RESEARCH CENTER	Strife	J. R.	East Hartford	CT	06108
UNITED TECHNOLOGIES-CSD	Ellis	Russ	San Jose	CA	95161-9028
UNITED TECHNOLOGIES-CSD	Mills	Edward R.	San Jose	CA	95161-9028
UNIVERSITY OF CALIFORNIA	Sines	George	Los Angeles	CA	90024
UNIVERSITY OF DELAWARE	Chou	Tsu-Wei	Newark	DE	19716
UNIVERSITY OF ILLINOIS AT CHICAGO	Chudnovsky	A.	Chicago	IL	60680
UNIVERSITY OF OKLAHOMA	Bert	C. W.	Norman	Oklahoma	73019
UNIVERSITY OF WASHINGTON	Fischbach	D.	Seattle	WA	98195
UNIVERSITY OF WYOMING	Adams	D. F.	Laramie	WY	82071
VIRGINIA POLYTECHNIC INSTITUTE	Hasselman	D. P. H.	Blacksburg	VA	24061
VIRGINIA POLYTECHNIC INSTITUTE	Jones	Robert M.	Blacksburg	VA	24061
VIRGINIA POLYTECHNIC INSTITUTE &	Reifsnider	K. L.	Blacksburg	VA	24601
VOUGHT CORPORATION	Volk	H.	Dallas	TX	75211
WILLIAMS INTERNATIONAL	Cruzen	Scott	Walled Lake	MI	48088

TOTAL

Printed 134 of the 147 records.

END
DATED
FILM
8-88
DTIC